THE EFFECT OF COMMON PREDICTABLE SURFACE ERRORS ON THE RADIATION PATTERN OF A PARABOLOID

A THESIS

Presented to

the Faculty of the Graduate Division

by

Woodson Dale Wynn

In Partial Fulfillment

of the Requirements for the Degree

Master of Science in Electrical Engineering

Georgia Institute of Technology

June 1961

THE EFFECT OF COMMON PREDICTABLE SURFACE ERRORS ON THE RADIATION PATTERN OF A PARABOLOID

Approved:

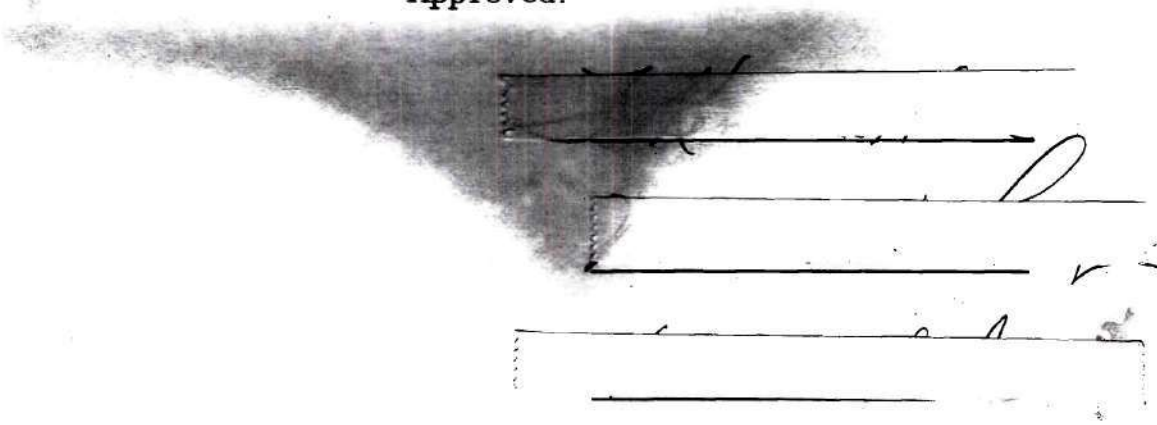

Date Approved by Chairman: April 12, 1961

"In presenting the dissertation as a partial fulfillment of the requirements for an advanced degree from the Georgia Institute of Technology, I agree that the Library of the Institution shall make it available for inspection and circulation in accordance with its regulations governing materials of this type. I agree that permission to copy from, or to publish from, this dissertation may be granted by the professor under whose direction it was written, or, in his absence, by the dean of the Graduate Division when such copying or publication is solely for scholarly purposes and does not involve potential financial gain. It is understood that any copying from, or publication of, this dissertation which involves potential financial gain will not be allowed without written permission.

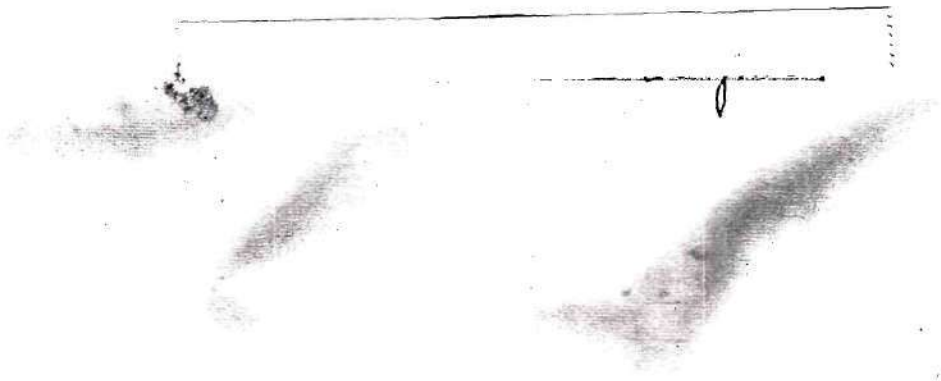

ACKNOWLEDGMENTS

The work herein described was made possible by use of the facilities of Scientific-Atlanta, Inc., Atlanta, Georgia. The contributions to the work by my thesis advisor, Dr. F. Kenneth Hurd, and by Mr. J. Searcy Hollis and other members of the staff of Scientific-Atlanta, Inc., are gratefully acknowledged.

TABLE OF CONTENTS

TABLE OF CONTENTS (Continued)

TABLE OF CONTENTS (Continued)

LIST OF TABLES

LIST OF ILLUSTRATIONS

SUMMARY

The purpose of this investigation was to illustrate a technique for computing, without difficulty, useful approximations of the far-field radiation patterns produced by paraboloidal antennas when subjected to known distortions. The technique is applicable if the reflector of an antenna is both large and smooth compared with the wavelength of radiated energy and if the distortions in the antenna are small compared with the edge diameter of the paraboloidal reflector.

For an antenna that satisfies the specified conditions, the method of geometrical optics is found particularly useful in obtaining a suitable approximation of the antenna aperture field. The geometrical optics principle is also applicable to the computation of the aperture fields of distorted antennas other than those considered in the technique. However, the principle is particularly easy to apply to antennas that satisfy the requirements of the technique.

In general the aperture field and far-field radiation pattern of an antenna are related by the expression

$$\overline{A} = j\frac{kK_1}{R}\int_S \overline{F}(x,y)\, e^{-jkr\,(\vec{z}\cdot\vec{R}\,+\,\vec{z}\cdot\vec{p})}\, dS.$$

For a microwave antenna the radiation pattern is usually confined to a narrow region about the axis of the undistorted paraboloidal reflector. For this case the relation between the aperture field and far-field radiation pattern reduces to

$$\overline{A} = K \int_S \overline{F}(x,y)\, e^{jk(x \cos\theta + y \sin\phi)}\, dS.$$

An analog computer is discussed which can evaluate this integral without difficulty. The far-field pattern computed is in a graphical form.

As an illustration of the technique, the method of geometrical optics and the analog computer are used to compute the radiation patterns of some distorted antennas. The antenna distortions considered are assumed to have the gross characteristics of the distortions produced in a particular paraboloidal antenna when the reflector of this antenna is subjected to different wind loads. The loads considered are particular intensities of an on-axis wind and also particular intensities of an off-axis wind. The nature of the characteristic distortion is dependent on the incident direction of the wind load and the distortion magnitude is dependent on the load intensity. In each case, a family of radiation patterns is computed corresponding to the various magnitudes of antenna distortion. In both cases it is found that increasing the distortion magnitude corresponds to a transition of the radiation pattern away from the optimum pattern produced when no antenna distortion is present. For either case, an upper limit on the distortion can be determined for a specified criterion in the radiation pattern.

CHAPTER I

INTRODUCTION

In the theory of microwave antennas it is shown that for a given amplitude illumination distribution in the antenna aperture, a uniform phase distribution over the aperture will give an optimum radiation pattern. A uniform phase distribution in the aperture of a paraboloidal antenna requires an exact parabolic surface when used with a point-source primary feed at the focal point of the reflector. Any deviations from this exact parabolic surface will introduce aperture phase errors which cause an increase in side-lobe level, deterioration of the sharpness of the pattern, and a decrease in gain of the main radiation beam. Severe phase errors may also cause the position of the main radiation beam to be shifted. In practice it is impossible to obtain the exact parabolic geometry desired due to the reflector surface deviations introduced in the manufacture and application of the antenna.

The surface deviations from a true paraboloidal reflector, that is, the surface errors, encountered are of two types. One type is systematic or predictable, and the other is random. Systematic surface errors and the antenna pattern deviations due to them are calculable by a complete and rigorous analysis of the problem. Examples of such systematic surface errors are sagging of the reflector under the force of gravity and the reflector distortion due to wind loading. On the other hand, random surface errors are caused by accidental and usually slight deviations of the reflector coordinates from their values in the

paraboloid of revolution. Into this class are placed machine errors and other random distortions of the paraboloidal reflector. The analysis of random surface errors is a statistical problem and is considerably different from an analysis of systematic surface errors. One method of solution for the problem of the effect of random surface errors in a paraboloidal antenna reflector on the radiation pattern has been given by Ruze (1).

In the case of systematic surface errors, it is theoretically possible to predict the coordinates for the distorted reflector surface. Therefore, if the phase and amplitude expressions for the primary feed are known, it is possible, in theory, to compute the phase and amplitude distributions in the antenna aperture field. From this aperture field the far-field radiation pattern can be computed.

The difficulty that is encountered in the determination of the far-field radiation patterns produced by systematically distorted paraboloidal antennas lies in the prohibitive mathematical analysis involved. This difficulty has limited the analysis of systematically distorted paraboloidal antennas. It was the purpose of this study to illustrate a technique of general applicability which yields a useful approximation to the solution without prohibitive mathematical analysis.

The technique will be applicable to those cases where

(1) The antenna distortions are known or can be approximated.

(2) The distortions are small in comparison with the dimensions of the antenna, and the distorted reflectors are both large and smooth compared with the wavelength of the radiated energy.

It will be shown that an accurate approximation of the aperture field for such distorted antennas can be computed without difficulty through the application of the method of geometrical optics. It will be shown also that the prohibitive calculations that may arise in computing the far-field radiation patterns from the aperture fields can be avoided by making use of special analog techniques.

The method will be illustrated by solving a specific problem, that of calculating the far-field radiation patterns of a paraboloidal antenna when it is subjected to certain wind loads. Of special interest will be the determination of the magnitude of these systematic antenna distortions which can be allowed for specified tolerances in the corresponding radiation pattern.

The method.--In Chapter II, a procedure is discussed for obtaining the approximate aperture field of a microwave antenna with a known reflector surface and a known point-source primary-feed amplitude distribution.

It is shown in Chapter III that the far-field radiation pattern, $\overline{A}(\theta,\phi)$,* of a narrow-beam microwave antenna can be expressed in terms of (a) its aperture energy distribution function $\overline{F}(x,y)$, and (b) the spherical coordinates θ and ϕ of the mathematical system used to derive the relation. Thus $\overline{A}(\theta,\phi)$ is given by

$$\overline{A}(\theta,\phi) = K\int_S \overline{F}(x,y)\, e^{jk(x\cos\theta + y\sin\phi)}\, dS \qquad (1)$$

---

*The superscribed bar will be employed to designate a complex quantity.

where $$K = j\frac{2kK_1}{R} e^{-jkR}.$$

A special analog computer which will solve Equation 1 for the narrow-beam far-field radiation pattern is discussed in Chapter IV.

In Chapter V, a procedure is discussed for relating known deviations in the reflector surface of a particular paraboloidal antenna to the narrow-beam far-field radiation pattern. It is shown that with this procedure the magnitude of the reflector distortions that can be allowed for specified radiation pattern tolerances can be determined.

CHAPTER II

THE GEOMETRICAL OPTICS APPROXIMATION

Huygen's principle (2) can be derived from Maxwell's equations which are known to relate any electromagnetic field to the sources producing that field. The principle states that if a source of radiation is completely enclosed by an imaginary surface and if the electromagnetic field is known at all points on the surface, the field at points exterior to the surface can be determined by summing the contributions to the field at the exterior points from each elemental area of the surface, by assuming each to be a secondary source of radiation. The summation is obtained by integration over the closed surface taking into account the amplitudes, phases, and polarizations of the fields over the closed surface.

Huygen's principle is particularly useful in solving antenna problems when a certain amount of specialization can be made as to the surface assumed to enclose the source of radiation. For the usual narrow-beam high-gain antenna, almost all the energy is radiated through a portion of the enclosing surface, and for this case a special surface configuration can be used which facilitates the solution. Since the closed surface can assume any arbitrary shape, it may be made such that the active portion, that is the portion through which most of the radiated energy passes, is a plane surface, say S. This surface is called the aperture of the antenna Since it was postulated that almost

all of the radiated energy passes through the aperture, the remaining part of the closed surface can be neglected in the integration process without introducing significant error in the calculation of the radiated field at points outside the surface. The plane surface provides a convenient geometry for the integration process involved. Also, it is relatively easy to obtain a close approximation to the field over the planar aperture by use of geometrical optics.

The geometrical optics principle can be explained by considering the usual microwave antenna. The field at a point in the antenna aperture consists of the sum of the primary feed field and the re-radiated field due to currents induced in the reflector surface by the radiation field of the primary feed. The former can usually be neglected if the primary feed energy is directed onto the reflector. The re-radiated field is the sum of contributions of elemental currents over the entire reflector, added vectorially. But the resultant field at any particular point in the aperture is, for the most part, due to a certain portion of the reflector from which the field contributions in the aperture arrive with essentially the same phase. This portion of the reflector is called "the region of constant phase" for the particular aperture point in question (3). For wavelengths that are large relative to the reflector dimensions, the region of constant phase may include almost the whole reflector. As the frequency of radiation is increased, the region of contribution becomes smaller. For optical frequencies the region of constant phase of a typical reflector is extremely small, and as the wavelength approaches zero, the field at a point in the aperture appears to be reflected from one point of the reflector. In this limit, lines

which are normal to phase fronts of the radiated energy and which join the reflection point and the feed are called "rays". In the geometrical optics method, radiant energy is assumed to propagate along such rays, which are straight lines in a homogeneous medium (4). Also, these rays exhibit equal angles of incidence and reflection at reflecting surfaces.

The intensity of the reflected field in the antenna aperture is obtained by applying the principle of conservation of energy to the total power contained in an incident cone of rays and the total power contained in the associated reflected pencil of rays that intersect the aperture (5). The phase of the aperture field of the antenna may be found with respect to the phase of a point source primary antenna feed by determining the optical path lengths of rays from the primary feed to the reflector and out to the aperture.

Strictly speaking, propagation by rays is valid only in the limit of zero wavelength; however, if the reflecting surface is both large and smooth compared with the wavelength, the field close to the surface is described quite closely by geometrical optics. For the usual microwave antenna this approximation is valid.

CHAPTER III

THE DERIVATION OF RELATIONS BETWEEN APERTURE-FIELD AND FAR-FIELD

Derivation of the general relation.--The electromagnetic field at any point P in the front hemisphere of Figure 1 due to diffraction through a large planar aperture of arbitrary shape is given (6) by the scalar equation

$$\overline{A} = K_1 \int_S \overline{F}(x,y) \frac{e^{-jkr}}{r} \left[\left(jk + \frac{1}{r} \right) \vec{z} \cdot \vec{r} + jk \vec{z} \cdot \vec{p} \right] dS \qquad (2)$$

where:

$\overline{F}(x,y)$	is a phasor, defined only in the x-y plane, which describes the amplitude and phase of the field over the aperture S.
λ	is the wavelength of the radiated energy.
k	is $\frac{2\pi}{\lambda}$.
$\vec{r}$, $\vec{R}$, $\vec{z}$, and $\vec{p}$	are unit vectors, the direction of $\vec{p}$ being the direction of power flow at the point (x, y) of the aperture.
K_1	is a constant of proportionality.

If, as is usually the case, the points P that are of interest are in the far-field of the aperture, the following simplifying assumptions can be made:

1. The distance r, except in the phase term e^{-jkr}, can be replaced by R, the distance from the field point to the

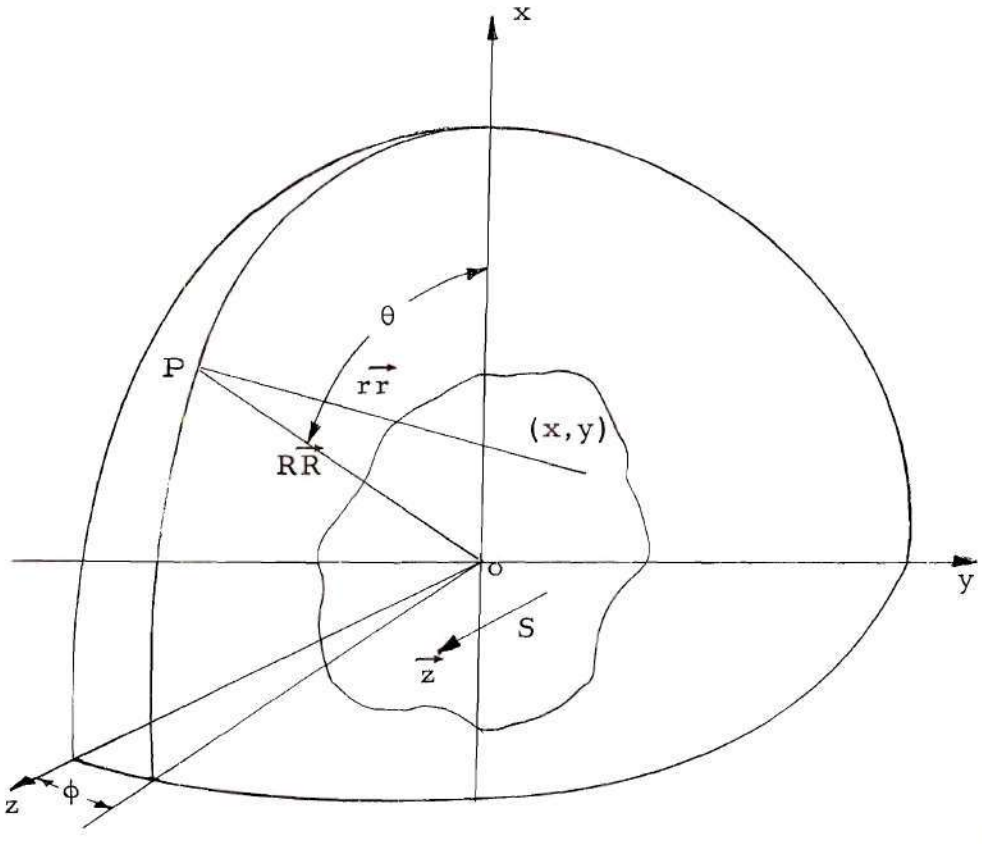

Figure 1. Aperture and Diffraction-Field Geometry

origin (which should be located in or near the aperture).

2. The term $1/r$ can be neglected in comparison with k.
3. The directions of r and R with respect to the z-axis can be considered equal and thus allowing $\vec{z}\cdot\vec{r}$ to be replaced by $\vec{z}\cdot\vec{R}$.

Equation 2 then becomes

$$\overline{A} = j\frac{kK_1}{R}\int_S \overline{F}(x,y)\, e^{-jkr}\left(\vec{z}\cdot\vec{R} + \vec{z}\cdot\vec{p}\right) dS. \tag{3}$$

The narrow beam approximation.--For a given aperture, the narrowest possible beamwidth is obtained when the energy distribution over the aperture is constant in both amplitude and phase (7). Thus, if the beam is to be confined to a narrow angular region near the z-axis, the phase over the aperture, $\psi(x,y)$, cannot vary greatly, and the factor $\left(\vec{z}\cdot\vec{R} + \vec{z}\cdot\vec{p}\right)$ can be replaced by its maximum value, 2. Equation 3 then becomes

$$\overline{A} = j\frac{2K_1k}{R}\int_S \overline{F}(x,y)\, e^{-jkr}\, dS. \tag{4}$$

It is found by expressing r in terms of R and dropping terms of higher order than the first, that for large distances

$$r \cong R - x\cos\theta - y\sin\phi. \tag{5}$$

Substitution of Equation 5 into Equation 4 gives

$$\overline{A} = K\int_S \overline{F}(x,y)\, e^{jk(x\cos\theta + y\sin\phi)}\, dS \tag{6}$$

where $$K = j\frac{2K_1 k}{R} e^{-jkR}.$$

For the aperture S shown in the x-y plane in Figure 2, Equation 6 is equal to either of the integrals

$$\overline{A} = K \int_{-a}^{+a} \left[\int_{-b}^{+b} \overline{F}(x,y)\, e^{jkx \cos\theta}\, dx \right] e^{jky \sin\phi}\, dy \qquad (7)$$

or $$\overline{A} = K \int_{-b}^{+b} \left[\int_{-a}^{+a} \overline{F}(x,y)\, e^{jky \sin\phi}\, dy \right] e^{jkx \cos\theta}\, dx. \qquad (8)$$

The general method of attack used to evaluate either of the integrals is to reduce the aperture to an "equivalent slit" aperture which is defined below.

Exploration of the radiation pattern in the y-z plane can be made by substituting $\theta = \pi/2$ for successive fixed values of y in Equation 7. With the substitution of $\overline{f}(y, \theta = \pi/2) = \int_{-b}^{+b} \overline{F}(x,y)\, dx$ which may be called $\overline{f}(y)$, Equation 7 becomes

$$\overline{A} = K \int_{-a}^{+a} \overline{f}(y)\, e^{jky \sin\phi}\, dy. \qquad (9)$$

This is a Fourier integral (8) which describes the solution of the two dimensional single slit diffraction problem.

It can be seen that a similar equivalent slit function can be obtained for values of θ other than $\pi/2$ by letting

$$\overline{f}(y, \theta_n) = \int_{-b}^{+b} \overline{F}(x,y)\, e^{jkx \cos\theta_n}\, dx. \qquad (10)$$

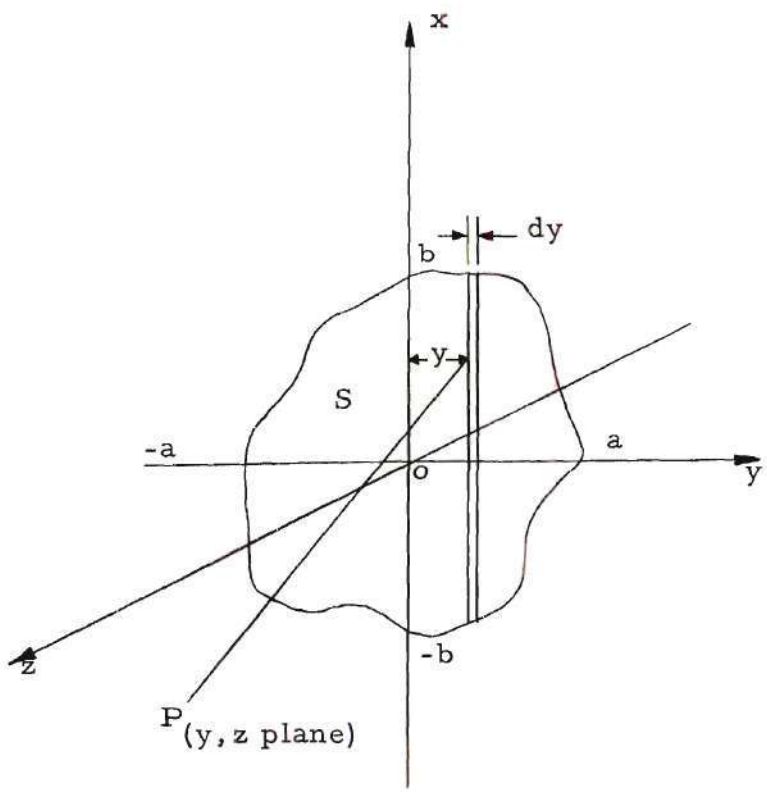

Figure 2. Aperture and Far-Zone Diffraction-Field Geometry

In this manner the radiation field from an aperture with a general distribution can be presented by means of a succession of ϕ cuts at fixed values of θ. The same pattern can be presented as a succession of θ cuts at fixed values of ϕ by using Equation 8 instead of Equation 7.

Equations 7 and 8 may be put into a useful normalized form, from the standpoint of the analog techniques to be presented in Chapter IV, as follows. If u and v are defined as

$$u = k a \sin \phi_n \tag{11}$$

and

$$v = k b \cos \theta_n \tag{12}$$

and if $y' = y/a$; $x' = x/b$, and constants of proportionality are dropped; Equation 7 can be written as

$$\overline{A}(u,v) = \int_{-1}^{+1} \overline{f}(y', \theta_n)\, e^{juy'} dy' \tag{13}$$

where

$$\overline{f}(y', \theta_n) = \int_{-1}^{+1} \overline{F}(x', y')\, e^{jvx'} dx',$$

and Equation 8 can be written as

$$\overline{A}(u,v) = \int_{-1}^{+1} \overline{f}(x', \phi_n)\, e^{jvx'} dx' \tag{14}$$

where

$$\overline{f}(x', \phi_n) = \int_{-1}^{+1} \overline{F}(x', y')\, e^{juy'} dy'.$$

Discussion of approximations and limitations.--The approximations contained in the derivation of Equation 3 are the common far-field

approximations and no appreciable error is incurred as a result of them (9). Equation 3 is general and applicable to problems where the radiation patterns cover wide angular regions. Equation 6 is a close approximation of Equation 3 when the far-field radiation pattern is confined to a small angular region about the z-axis.

There is no sharp transition between problems in which Equation 6 may be used and those in which Equation 3 must be used. In the transition region the selection of one equation over the other will be primarily dependent on the desired accuracy in the predicted radiation pattern. Past results have indicated that the shape of the far-field pattern is relatively insensitive to small variations in the aperture amplitude function, and that Equation 6 may usually be used if the radiation pattern is confined to angles not greater than 30° (10).

CHAPTER IV

THE FOURIER INTEGRAL ANALOG COMPUTER

Evaluation of the Fourier integral.--It has been shown (11) that analog computer techniques are applicable to the evaluation of the Fourier integral

$$\overline{A}(u,v) = \int_{-1}^{+1} \overline{f}(y', \theta_n)\, e^{juy'}\, dy' \qquad (15)$$

which expresses the desired transformation between the normalized aperture distribution of a narrow-beam microwave antenna and its far-zone radiation pattern. In this chapter a special analog computer* is described which provides graphical solutions to the Fourier integral.

The analog computer automatically evaluates $\overline{A}(u,v)$ from an equation of the form 13 or 14 generating a succession of cuts in u or v. Such a family of cuts defines the spatial radiation pattern described previously. For the general two-dimensional aperture, the computer is also used to find an equivalent slit aperture through evaluation of $\overline{f}(y', \theta_n)$ or $\overline{f}(x', \phi_n)$.

It is seen that the Fourier integrals $\overline{A}(u,v)$, $\overline{f}(y', \theta_n)$, and $\overline{f}(x', \phi_n)$ are identical in form. For this reason a general integral is defined in terms of a machine variable X and a machine parameter U as follows

---

*The Model CF 1 Fourier Integral Computer produced by Scientific-Atlanta, Inc., Atlanta, Georgia.

$$I(U) = \int_{-1}^{+1} \overline{F}(X)\, e^{jUX}\, dX \qquad (16)$$

or

$$I(U) = \int_{-1}^{+1} \overline{F}(X)\, e^{j\left[\psi(X) + UX\right]}\, dX \qquad (17)$$

where

$$\overline{F}(X) = F(X)\, e^{j\psi(X)}.$$

The block diagram in Figure 3 indicates the method of evaluating the general integral 17 in the analog computer. The amplitude function F(X) and the phase function $\psi(X)$ are drawn in ink on a special dual graph paper. These curves are attached to a drum of a graph-reading function generator with X-axis parallel to the axis of the drum. As the drum rotates at 3600 rpm, two synchronized photoelectric readers scan the curves along the X-axis. In every drum revolution, the passing of each curve over its photoelectric reader generates a pulse with a time position that is a measure of the function magnitude. Two pulse-position to voltage converters generate varying direct voltages with waveforms that are reproductions of the amplitude and phase functions drawn on the graphs. A complete traverse of the X-axis is made in four seconds, so that each function is sampled at 240 points.

The phase argument of the integrand of Equation 17 is the sum of the phase function $\psi(X)$ and the product UX. A precision 10-turn helical potentiometer develops a voltage proportional to the parameter U, and this voltage is integrated to produce a linearly rising ramp with an instantaneous amplitude that is proportional to UX. A summation

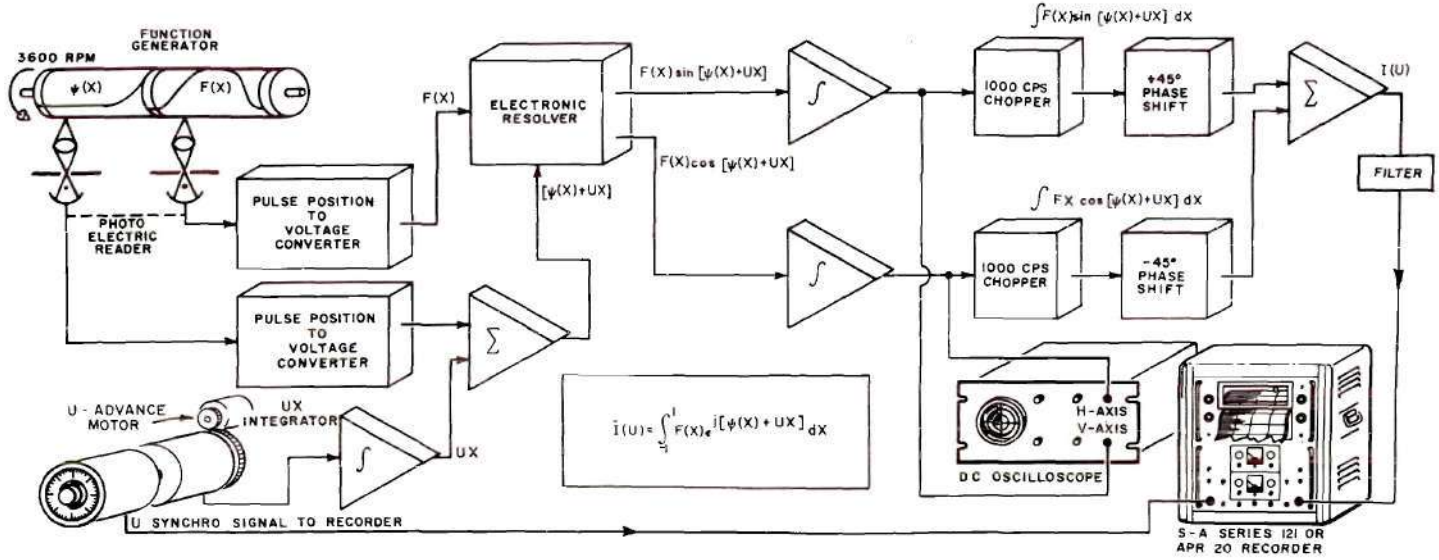

Figure 3. Simplified Block Diagram of Model CF 1 Fourier Integral Computer

circuit produces the total phase argument $\Psi(X) + UX$. Geared to the U potentiometer is a synchro transmitter which controls the chart position of an integral magnitude recorder*, and a motor which can automatically advance U after each four-second integration period.

An electronic resolver performs the conversion

$$F(X)\, e^{j\left[\Psi(X) + UX\right]} = F(X) \cos\left[\Psi(X) + UX\right] + jF(X) \sin\left[\Psi(X) + UX\right] . \tag{18}$$

The two quadrature components of the integrand are introduced into chopper-stabilized electronic integrators which evaluate the corresponding components of the integral between the ±1 limits of X. After integration the quadrature signals are converted to one-kilocycle sine-wave voltages and are added in phase quadrature to produce an output which is proportional to I(U).

A complex-plane plot of the integral is displayed by means of a long persistence oscilloscope. This display provides a means of reading the phase of the solution and is also of value in studying the generation of the solution.

Each integration cycle of the circuit establishes one point in the solution. The magnitude of the solution for each integration cycle is recorded on the integral magnitude recorder and the phase is read from the oscilloscope. By repeating the cycle of integration with U

---

*An Antenna Pattern Recorder produced by Scientific-Atlanta, Inc., is used.

advanced each cycle, a plane cut of the radiation pattern of the normalized aperture is obtained from the amplitude and phase functions of the normalized aperture equivalent slit.

To convert the two-dimensional normalized aperture to an equivalent slit, a single-cycle mode of operation in the computer is used. The curves of the integrands of $\overline{f}(y', \theta_n)$ or $\overline{f}(x', \phi_n)$ for successive values of x' or y' are attached to the computer drum, and the corresponding values of the integral are recorded in both phase and magnitude. The integral values for successive values of x' or y' are points on the curves of the corresponding phase and amplitude functions of $\overline{f}(y', \theta_n)$ or $\overline{f}(x', \phi_n)$.

Errors in the analog computer.--If the linear mode of operation is used in the magnitude recorder of the computer, the specified accuracy of the machine is one per cent of full-scale deflection of the recorder. If a logarithmic mode with 0 to 40 db range is used in the magnitude recorder, the specified accuracy of the machine is ±0.25 db for 0 to 10 db, ±0.5 db for 10 to 20 db, ±1.0 db for 20 to 30 db, ±2 db for 30 to 35 db, and ±3 db for 35 to 40 db (12). These results are based on the machine errors that can be introduced from the reading of a set of functions on the revolving drum to the recording of the corresponding integral.

Figure 4 shows a pattern computed by the analog computer for a 50 wavelength circular aperture with an equivalent slit aperture function with zero phase and constant magnitude. The stair-step curve shown in Figure 4 is the curve drawn by the computer amplitude

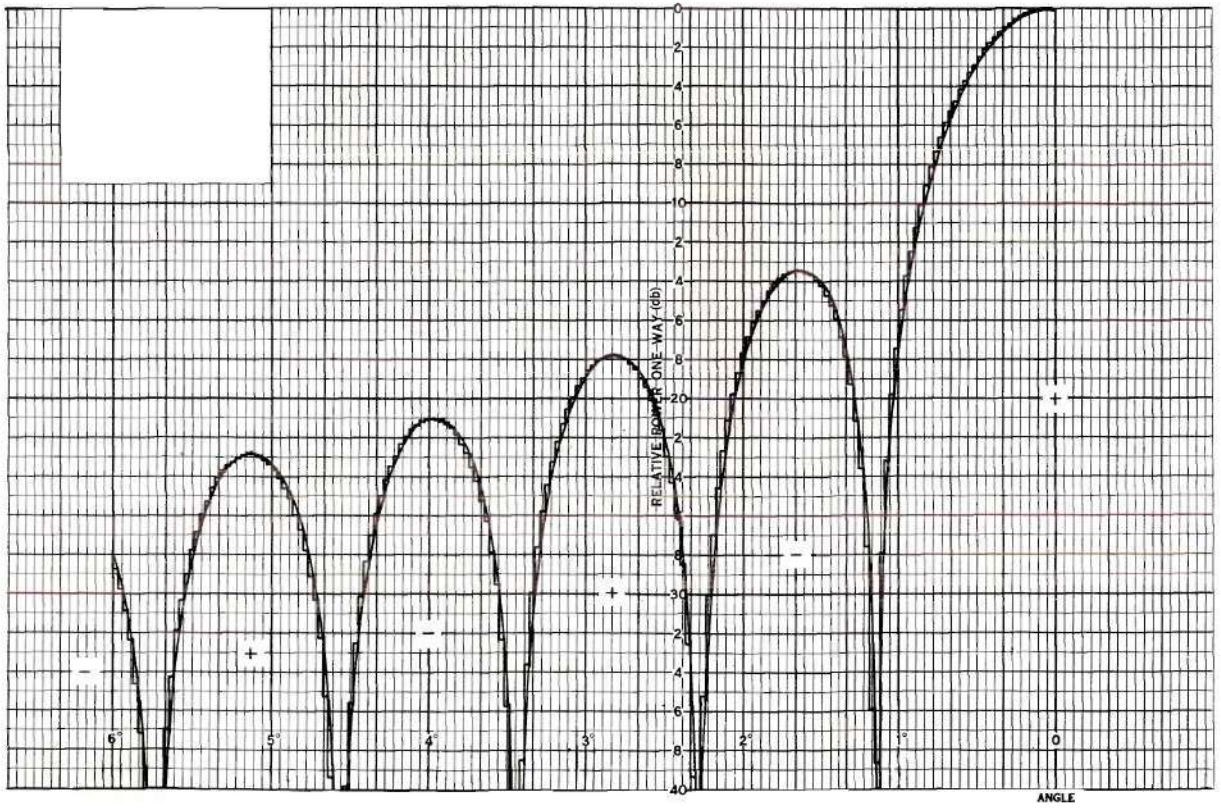

Figure 4. Computed Sin u/u Pattern

recorder. The righthand corner points of this curve are computed values of the pattern magnitude. The smooth envelope through the points of the computed values gives the computed pattern magnitude in decibels below zero. A plus or minus sign in a lobe of this recorded curve signifies that the lobe is either in phase or 180° out of phase with respect to the phase of the pattern at its peak magnitude.

It is well known that the far-field pattern corresponding to the specified equivalent slit aperture field function is a sin u/u pattern. Therefore, an idea of the accuracy of the computer with a 0 to 40 db logarithmic recorder can be obtained by comparing the smooth curve of Figure 4 with the sin u/u pattern corresponding to the 50 wavelength equivalent slit aperture.

CHAPTER V

PROCEDURE

As an illustration of a method that might be used to solve the problem of relating the systematic distortions of a paraboloidal antenna to the respective far-field radiation patterns produced, a particular antenna subjected to particular wind loads will be considered.

Characteristics of the antenna.--The antenna to be considered is assumed to have, among others, the following characteristics

1. The rim of the antenna reflector is 50 wavelengths in diameter, and it does not deviate in shape or position when the antenna is subjected to a wind load.
2. The point source primary feed for each distorted antenna is located at a distance of 20 wavelengths from the reflector on the line that is normal to the distorted surface at the surface point that would be the center of revolution of the surface with no distortion.
3. The point source primary feed has a field amplitude distribution such that the feed produces a Taylor Distribution (13) in the aperture field of the paraboloidal antenna (Appendix I).

The source of distortion.--The surface of the reflector is considered to be exposed to two particular directions of a wind load with different fixed intensities for each. For each intensity, the wind load is uniform in the plane perpendicular to its direction of motion.

For a particular direction and intensity of the wind load on the reflector surface, it would be possible in theory to calculate the antenna reflector distortion produced if the surface force distribution produced by the load could be determined and if sufficient information were known about the mechanical structure of the antenna. However, this problem would be difficult if not impossible to solve in practice.

For purpose of illustration, surfaces will be defined from consideration of the physical problem which are considered to have the gross characteristics of the antenna reflector when it is subjected to the sources of distortion. The locations of the primary feeds associated with these characteristic surfaces will be inferred from the primary characteristics assumed for the antenna. The relations between the characteristic antennas assumed and the respective far-field radiation patterns produced will be determined.

The distortions.--The reflector surfaces to be considered are those which are assumed to have the gross characteristics of the distorted antenna reflector surfaces which result when the antenna is exposed to the source of distortion with different intensities and with angles of incidence on the reflector of 0° and 45° with respect to the z-axis, as shown in Figures 5 and 6, respectively.

The surfaces selected as characteristic of the distorted reflectors in the 0° incidence case, denoted by Case I, are surfaces of revolution

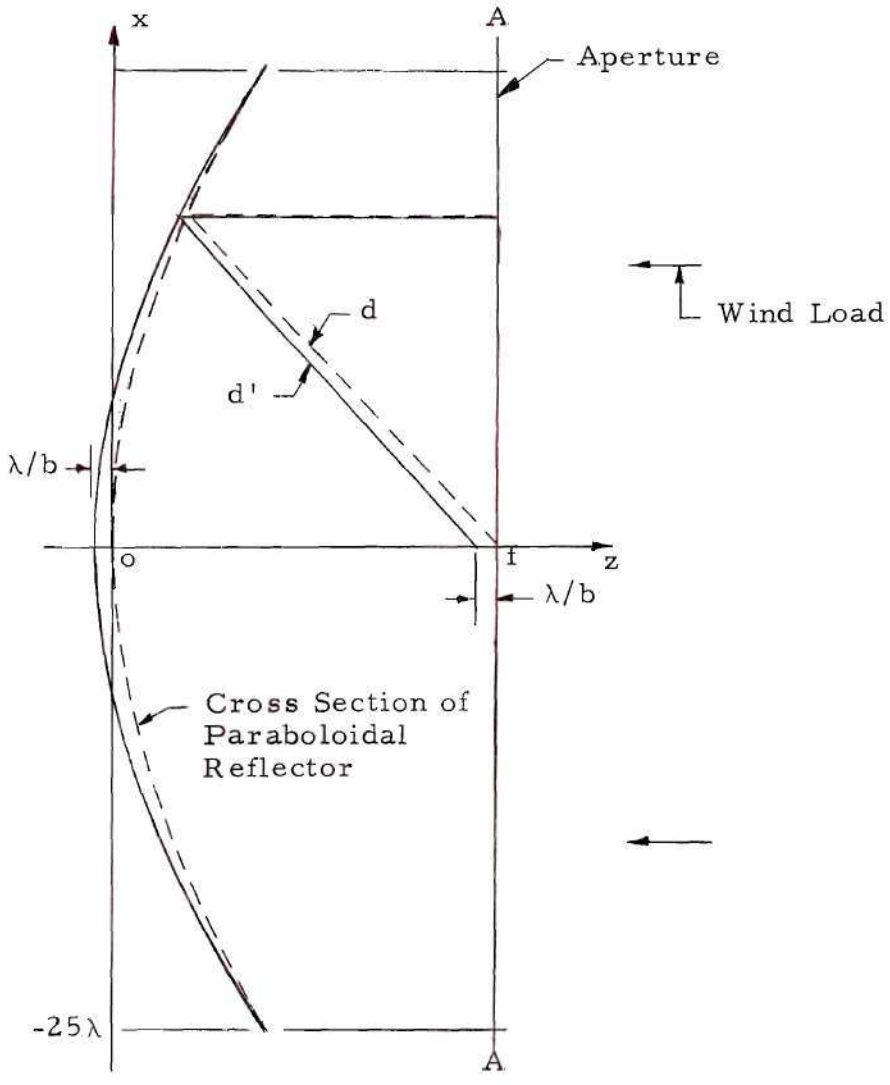

Figure 5. The Cross Section of the Distorted Antenna in Case I

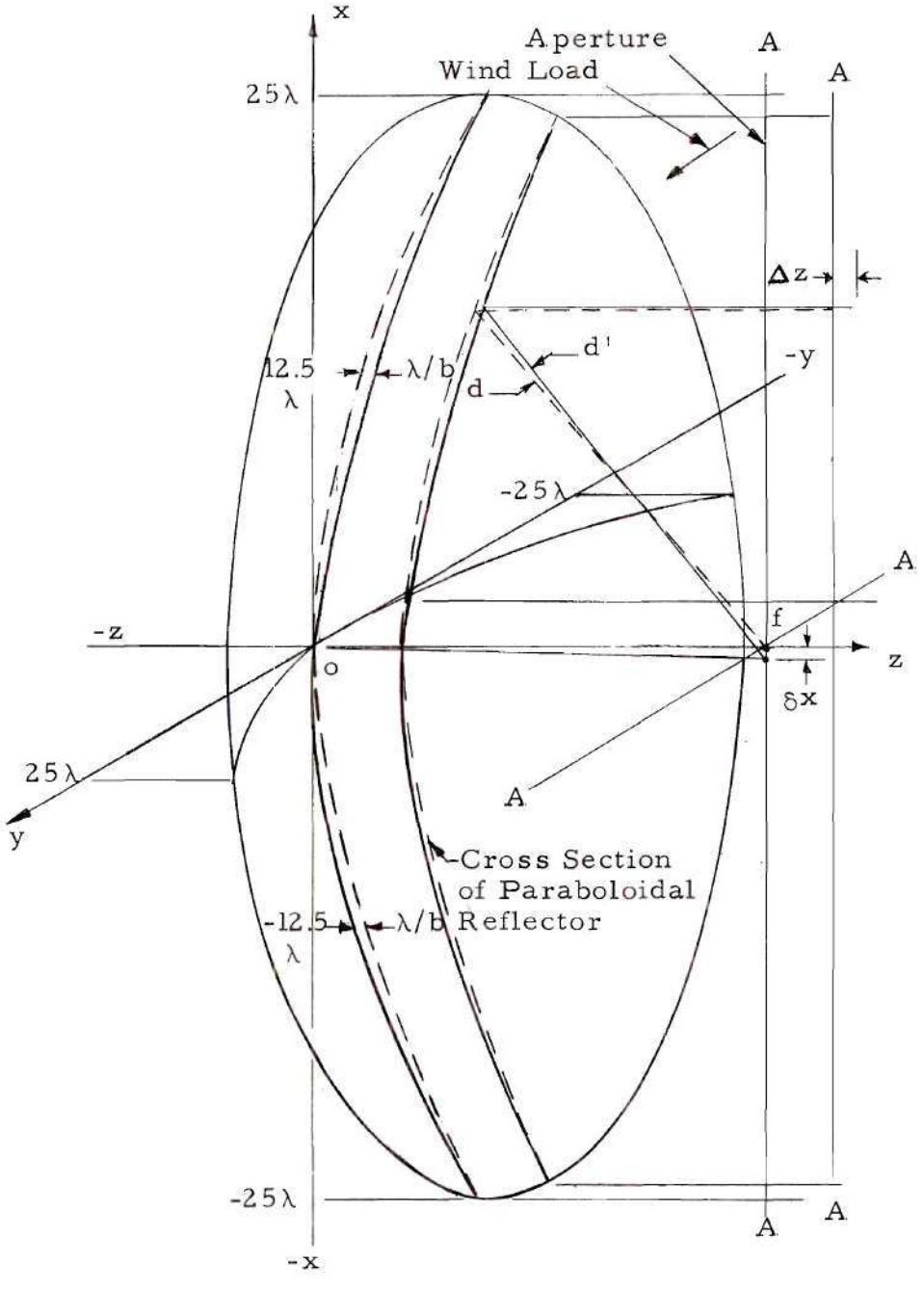

Figure 6. The Distorted Antenna in Case II

about the z-axis. The distorted reflectors selected are those obtained by moving each point of the paraboloidal surface in the negative z direction such that the distortion is maximum at the center of each reflector and decreases linearly with respect to radius to zero at the rim of the antenna. Referring to the reflector cross-sections in the x-z plane shown in Figure 5, the cross-sections are given by

$$z = \frac{x^2}{4f} + \frac{(0.04)|x|}{b} - \frac{\lambda}{b} \tag{19}$$

where λ is the wavelength of the radiated energy to be associated with the antenna,

$f = 20\lambda$,

$|x| \leq 25\lambda$,

and b is assigned positive values each of which is assumed to correspond to some intensity of the on-axis wind load.

The surfaces selected as characteristic of the distorted reflectors which would occur in the 45° incidence case, denoted by Case II, with the direction of incidence parallel to the x-z plane are as follows: For each surface, points on the paraboloidal surface are distorted in the +z direction for $x>0$ and in the -z direction for $x<0$ with magnitudes which are symmetrical about both the x-z and y-z planes. For a fixed value of y the distortion increases linearly with x from zero at $x = 0$ to a maximum at x midway between $x = 0$ and the x coordinate of the reflector rim. It then decreases linearly with x to zero at the reflector rim. The maximum distortion decreases linearly from a maximum value of λ/b at $y = 0$ to zero at $y = 25\lambda$. Referring to Figure 6, the

surfaces are given by

$$z = \frac{x^2 + y^2}{4f} - \left(\frac{2\lambda}{b}\right)\left(\frac{25\lambda - |y|}{25\lambda}\right)\left(1 + \frac{x}{625\lambda^2 - y^2}\right) \qquad (20)$$

for $$-\sqrt{625\lambda^2 - y^2} \leq x \leq -\sqrt{\frac{625\lambda^2 - y^2}{2}},$$

$$z = \frac{x^2 + y^2}{4f} + \left(\frac{2\lambda}{b}\right)\left(\frac{25\lambda - |y|}{25\lambda}\right)\left(\frac{x}{625\lambda^2 - y^2}\right) \qquad (21)$$

for $$0 \leq |x| \leq \sqrt{\frac{625\lambda^2 - y^2}{2}},$$

and $$z = \frac{x^2 + y^2}{4f} + \left(\frac{2\lambda}{b}\right)\left(\frac{25\lambda - |y|}{25\lambda}\right)\left(1 - \frac{x}{\sqrt{625\lambda^2 - y^2}}\right) \qquad (22)$$

for $$\frac{\sqrt{625\lambda^2 - y^2}}{2} \leq x \leq \sqrt{625\lambda^2 - y^2},$$

where $f = 20\lambda$,

$0 \leq |y| \leq 25\lambda$,

and b is assigned positive values each of which is assumed to correspond to some intensity of the 45° incident wind load.

In both Cases I and II it is seen that increasing the load intensities will correspond to decreasing the value of b.

The range of deviations introduced in the paraboloidal antenna reflector considered here is that range for which the maximum over-all

phase deviations in the aperture take on values from 0° to 180°. For the maximum over-all phase deviations in the aperture it will be found that b must be greater than 2.

The effects of the characteristic surface distortions introduced by Case I on the locations of the primary feed point of the antenna are assumed to be shifts of the feed point $-\lambda/b$ along the z-axis, as shown in Figure 5. The effects of the characteristic surface distortions introduced by Case II on the locations of the primary feed point of the antenna are assumed to be shifts of the feed point by $1.6\lambda/b$ in the negative x direction (Appendix II), as shown in Figure 6.

Computation of the aperture fields.--Because of the nature of the distorted antennas derived from the reflector deviations, certain simplifying assumptions will be made in calculating the antenna aperture field. The simplifying assumptions are:

(1) The reflector surfaces are both large and smooth in comparison with the wavelength of the radiated energy, and hence the method of geometrical optics may be used.

(2) The deviations of the distorted antennas will be small in comparison with the dimensions of the antenna. Therefore, the aperture field amplitude function will be approximately invariant with the antenna distortions; and the aperture field phase functions will be approximately those obtained by assuming that the optical paths of reflected rays will be parallel to the z-axis, as shown in both Figures 5 and 6.

The procedure used in finding the aperture field phase functions for the assumed distorted antennas will be demonstrated by finding the aperture field phase function for Case I.

The aperture phase function will be found in the plane at z = f as shown in Figures 5 and 6. For the case of the undistorted paraboloidal antenna, points that are 2f from the feed point along the reflected ray paths will lie in this plane. This implies that the plane is an equiphase plane, and the phase function for the aperture field of the paraboloidal antenna may be taken as zero.

If the antenna is distorted in the manner of Case I and if rays in the x-z plane of Figure 5 are traced from the feed point to the reflector and back parallel to the z-axis, the points on the rays that are 2f along the ray paths from the feed point will define an equiphase curve that can be used to determine the aperture field phase functions. The derivation of these phase functions is simplified by shifting the distorted antennas such that the center of revolution of each is at the origin, as shown in Figure 7. Letting z' be the z-coordinate in the x-z plane for the shifted antennas,

$$z' = \frac{x^2}{4f} + \frac{(0.04)\,|x|}{b} . \tag{23}$$

From Figure 7,

$$d' = \sqrt{(f - z')^2 + x^2} . \tag{24}$$

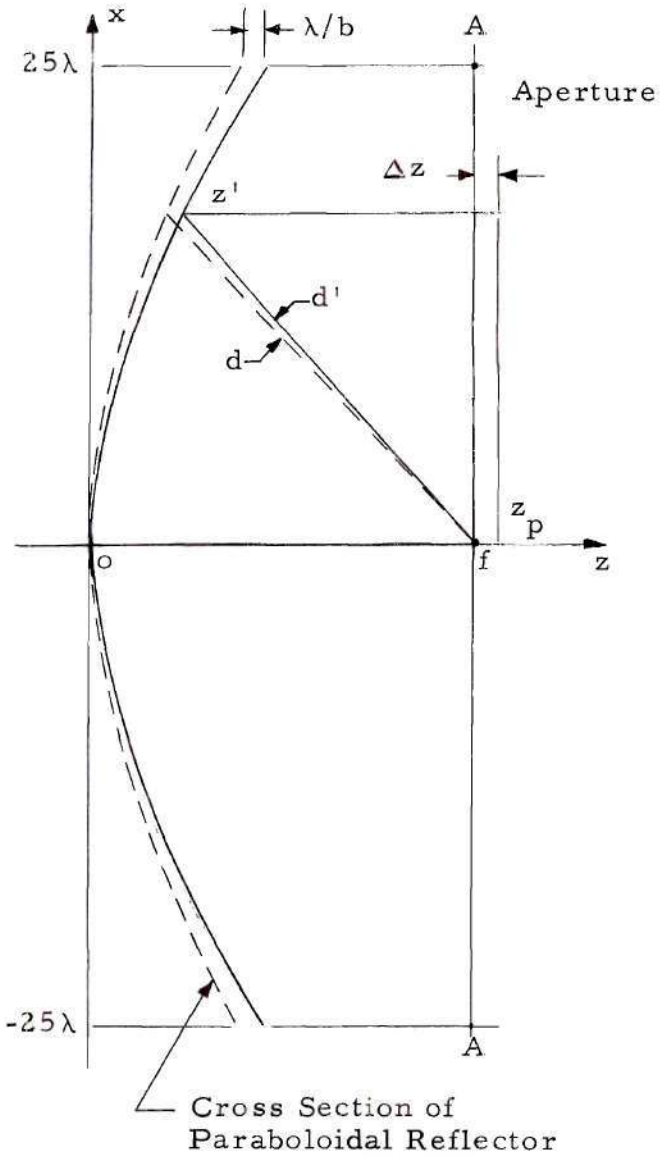

Figure 7. The Shifted Cross Section of the Distorted Antenna in Case I

Substituting Equation 23 into Equation 24,

$$d' = \left\{ \left[\left(f - \frac{x^2}{4f} \right)^2 + x^2 \right] + \left[\left(\frac{0.04|x|}{b} \right)^2 - \left(\frac{0.08|x|}{b} \right) \left(f - \frac{x^2}{4f} \right) \right] \right\}^{1/2} . \qquad (25)$$

In Figure 7,

$$d = \left[\left(f - \frac{x^2}{4f} \right)^2 + x^2 \right]^{1/2} \qquad (26)$$

where d is the distance from the focal point of the paraboloidal antenna reflector to any point on the x-z cross-section of the reflector. For the range between 0° and 180° in the magnitude of the maximum deviation in the aperture field phase function in Case I, the magnitude of the difference between d and d' must be less than $\lambda/2$. Then $d \cong d'$ for Equation 25, and d' may be approximated by the first two terms of the binomial expansion

$$(X + Y)^{1/2} = X^{1/2} + \frac{1}{2} X^{-1/2} Y + \frac{\left(\frac{1}{2}\right)\left(-\frac{1}{2}\right)}{2!} X^{-3/2} Y^2 + \text{---} \qquad (27)$$

where $$X = x^2 + \left(f - \frac{x^2}{4f} \right)^2 = \left(\frac{x^2}{4f} + f \right)^2 = d^2$$

and $$Y = \left[\left(\frac{0.04|x|}{b} \right)^2 - \left(\frac{0.08|x|}{b} \right) \left(f - \frac{x^2}{4f} \right) \right] .$$

Then $$d' \cong \left(\frac{x^2}{4f} + f \right) + \frac{\left[\frac{0.0016}{b^2} x^2 + \frac{0.02}{bf} |x|^3 - \frac{0.08f}{b} |x| \right]}{2\left(\frac{x^2}{4f} + f \right)} . \qquad (28)$$

From Figure 7

$$z_p = z' + 2f - d' \qquad (29)$$

defines an equiphase curve. The phase deviations in the aperture, with respect to zero phase of the true paraboloidal antenna, can be found from

$$\Delta z = z_p - f = z' + f - d' \tag{30}$$

when Δz is converted to degrees of phase in the aperture (phase deviation in degrees is $360\,\Delta z/\lambda$. Substituting Equations 23 and 28 into Equation 30,

$$\Delta z \cong \frac{\frac{0.32}{b} f^2 |x| + \frac{0.0032f}{b^2} x^2}{x^2 + 4f^2}. \tag{31}$$

The upper and lower limits of the righthand side of 31 occur at $|x| = 0$ and $|x| = 25\lambda$ respectively. For a maximum phase deviation of 180° in the antenna aperture, Δz must be $\lambda/2$. For $\Delta z \leqq \lambda/2$, it is found by considering the first term alone in the numerator of Equation 31 that the minimum of b is approximately 2.876. From this it follows that

$$\frac{\frac{0.0032\,fx^2}{b^2}}{\frac{0.32\,f^2|x|}{b}} << 1 \tag{32}$$

for $\Delta z \leqq \lambda/2$

and $0 \leqq |x| \leqq 25\lambda$

where $f = 20\lambda$.

Thus,
$$\Delta z \cong \frac{1}{b}\left(\frac{128\lambda^2|x|}{x^2 + 1600}\right) \tag{33}$$

for
$$0 \leqq |x| \leqq 25\lambda$$

and
$$b \geqq 2.876$$

where $b \cong 2.876$ produces a maximum magnitude of deviation of 180° in the aperture field phase function.

In a similar manner the expression is found (Appendix III) from which the aperture field phase functions can be computed, with respect to the zero aperture phase produced by the paraboloidal antenna, for the distorted antennas from Case II. The function computed for Case II is

$$\Delta z \cong \frac{\frac{16\lambda f^2}{b}\left(\frac{x}{25\lambda}\right)\sqrt{\frac{25\lambda - |y|}{25\lambda + |y|}} + 4fx\left(-\frac{1.6\lambda}{b}\right)}{x^2 + y^2 + 4f^2} \tag{34}$$

where
$$f = 20\lambda,$$

$$0 \leqq |x| \leqq \frac{\sqrt{625\lambda^2 - y^2}}{2},$$

$$b \geqq 5.76,$$

and
$$0 \leqq |y| \leqq 25\lambda,$$

$$\Delta z \cong \frac{-\frac{1}{b}\,16\lambda f^2\left[\left(\frac{x}{25\lambda}\right) + \frac{\sqrt{625\lambda^2 - y^2}}{25\lambda}\right]\sqrt{\frac{25\lambda - |y|}{25\lambda + |y|}} + 4fx\cdot\delta x}{x^2 + y^2 + 4f^2} \tag{35}$$

where $f = 20\lambda$,

$$-\sqrt{625\lambda^2 - y^2} \leqq x \leqq -\sqrt{\frac{625\lambda^2 - y^2}{2}},$$

$$b \geqq 5.76,$$

$$0 \leqq |y| \leqq 25\lambda,$$

and
$$\Delta z \cong \frac{\frac{1}{b}\,16\lambda f^2\left[\frac{\sqrt{625\lambda^2 - y^2}}{25\lambda} - \left(\frac{x}{25\lambda}\right)\right]\sqrt{\frac{25\lambda - |y|}{25\lambda + |y|}} + 4fx\cdot\delta x}{x^2 + y^2 + 4f^2} \tag{36}$$

where $f = 20\lambda$

$$b \geqq 5.76$$

$$0 \leqq |y| \leqq 25\lambda$$

$$\sqrt{\frac{625\lambda^2 - y^2}{2}} \leqq x \leqq \sqrt{625\lambda^2 - y^2}\ .$$

Specific magnitudes of reflector distortion for Cases I and II.--Two sequences of approximate values are selected for b such that the maximum deviation of the aperture field phase function in both Case I and Case II has the sequence of values 0°, 5.625°, 11.25°, 22.5°, 45°, 90°, and 180°. For Case I the required sequence of values for b are respectively ∞, 32 x 2.876, 16 x 2.876, 8 x 2.876, 4 x 2.876, 2 x 2.876, and 2.876; and for Case II the values for b are respectively ∞, 32 x 5.76, 16 x 5.76, 8 x 5.76, 4 x 5.76, 2 x 5.76, and 5.76 (Appendix IV). The six values of b in Case I or Case II will produce,

from Equation 33 or Equations 34, 35, and 36 six aperture-field phase functions which with the assumed aperture-field amplitude function will produce six far-field radiation patterns. Each of the two sequences of patterns then may be compared with the pattern computed for the undistorted antenna. For both Case I and Case II the changing characteristics of the radiation patterns with respect to the optimum pattern may be compared with the corresponding values assigned to b.

The pattern cuts considered.--Planar cuts of the far-field radiation patterns produced by the aperture field functions for Case I and Case II were computed by means of the analog computer discussed in Chapter IV.* For Case I, the radiation pattern is symmetrical about the z-axis and hence, the pattern computed in the x-z plane of Figure 5 is sufficient to describe the entire far-field radiation pattern. However, for Case II many cuts are necessary to describe the far-field radiation pattern in detail. For Case II some important characteristics of the effect of the reflector distortion magnitude on the far-field radiation pattern are shown by computing the radiation patterns in the x-z and y-z planes of Figure 6.

The determination of the equivalent slit apertures.--The phase and amplitude curves of the equivalent slit apertures used to compute the far-field radiation patterns in the x-z plane for Case I and in the x-z and y-z planes for Case II are formed by evaluating each equivalent slit aperture function at twenty points from the aperture field functions in

---

*The radiation patterns that are recorded here are field magnitudes only; the phase in the radiation patterns is not recorded.

twenty corresponding cuts equally spaced along the line of the equivalent slit in the aperture.

The data needed to compute the aperture field phase functions and the data for the equivalent slit aperture amplitude and phase functions are given in Appendix V and Appendix VI respectively.

The unnormalization of computer results.--All of the antenna apertures are put into a normalized form in order to program for the analog computer. The actual radiation patterns produced by the antennas are obtained from the computed patterns by use of the normalizing Equations 11 and 12.

CHAPTER VI

RESULTS

The narrow-beam far-field radiation patterns in the x-z plane of Figure 5 for Case I of the assumed reflector distortions with selected magnitudes of the distortion corresponding to $b = \infty$ and $b \cong 2^n \times 2.876$, $n = 0, 1, 2, 3, 4$, and 5 are shown in Figures 8 and 9. Figure 10 shows the far-field radiation patterns in the y-z plane of Figure 6 produced by the distorted antennas for Case II of the assumed reflector distortions where the magnitudes of reflector distortion correspond to $b = \infty$ and $b \cong 2^n \times 5.76$, $n = 0, 1, 2, 3, 4$, and 5. Figures 11 and 12 show the radiation patterns in the x-z plane of Figure 6 for Case II.

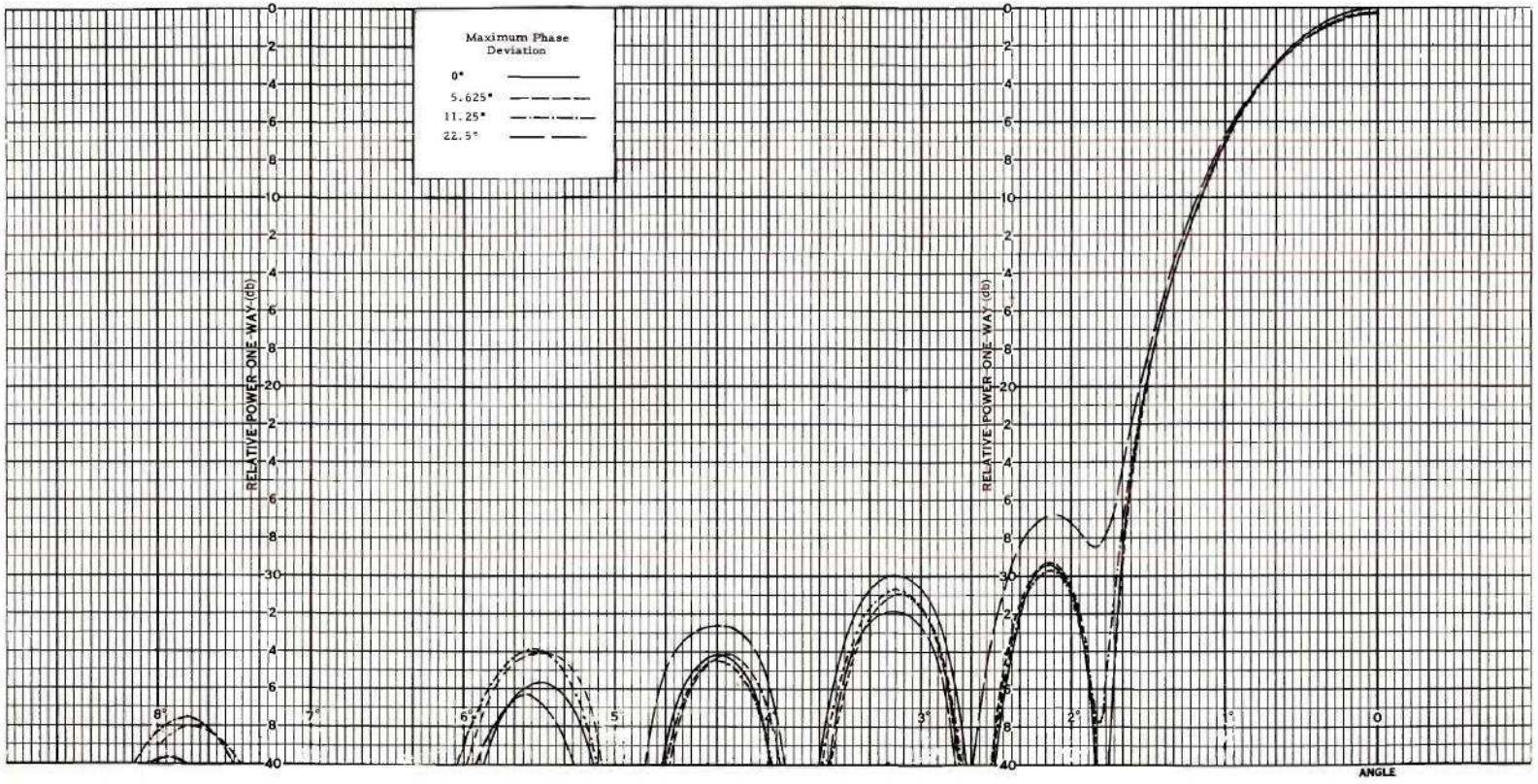

Figure 8. Patterns Computed for Case I

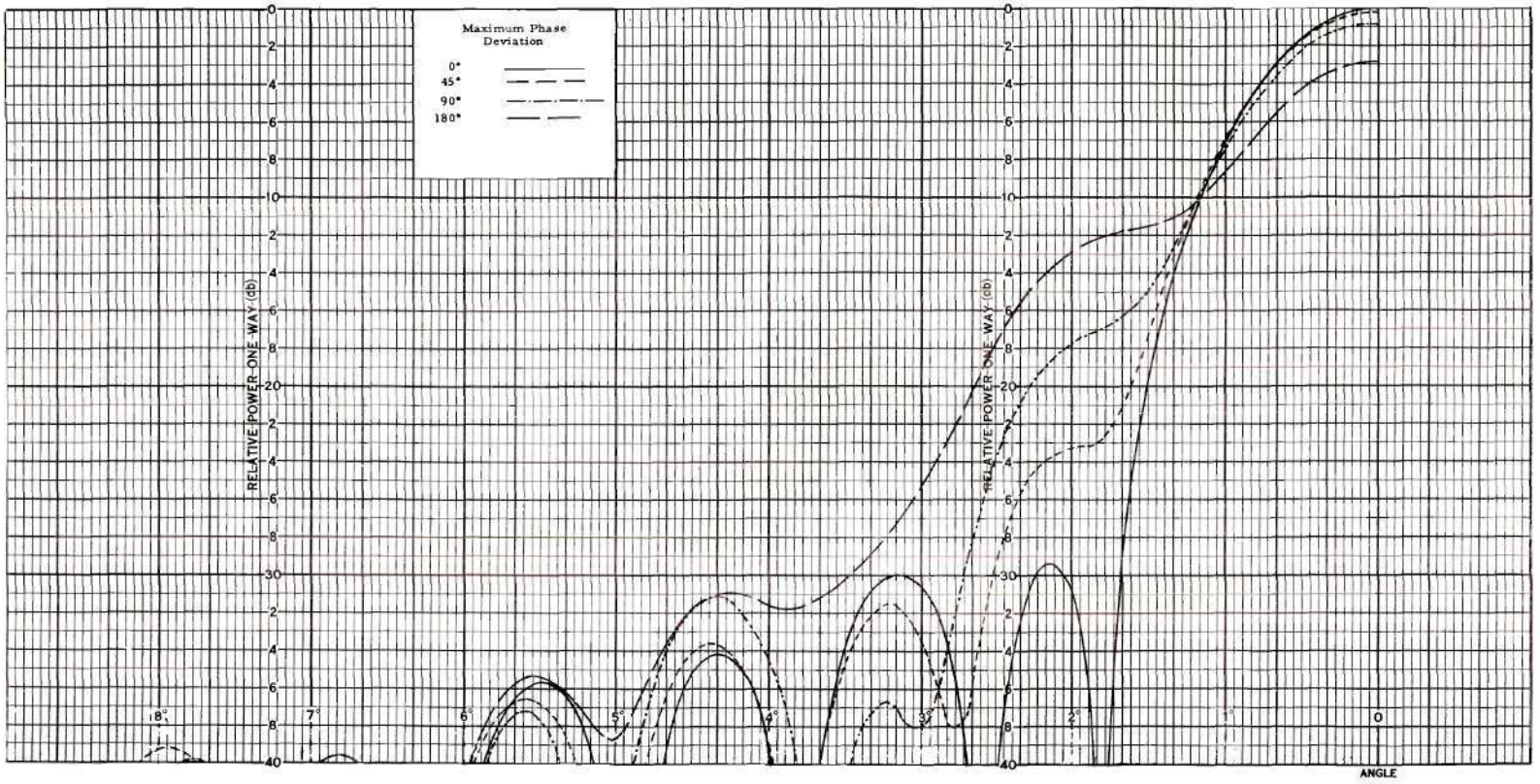

Figure 9. Patterns Computed for Case I (Continued)

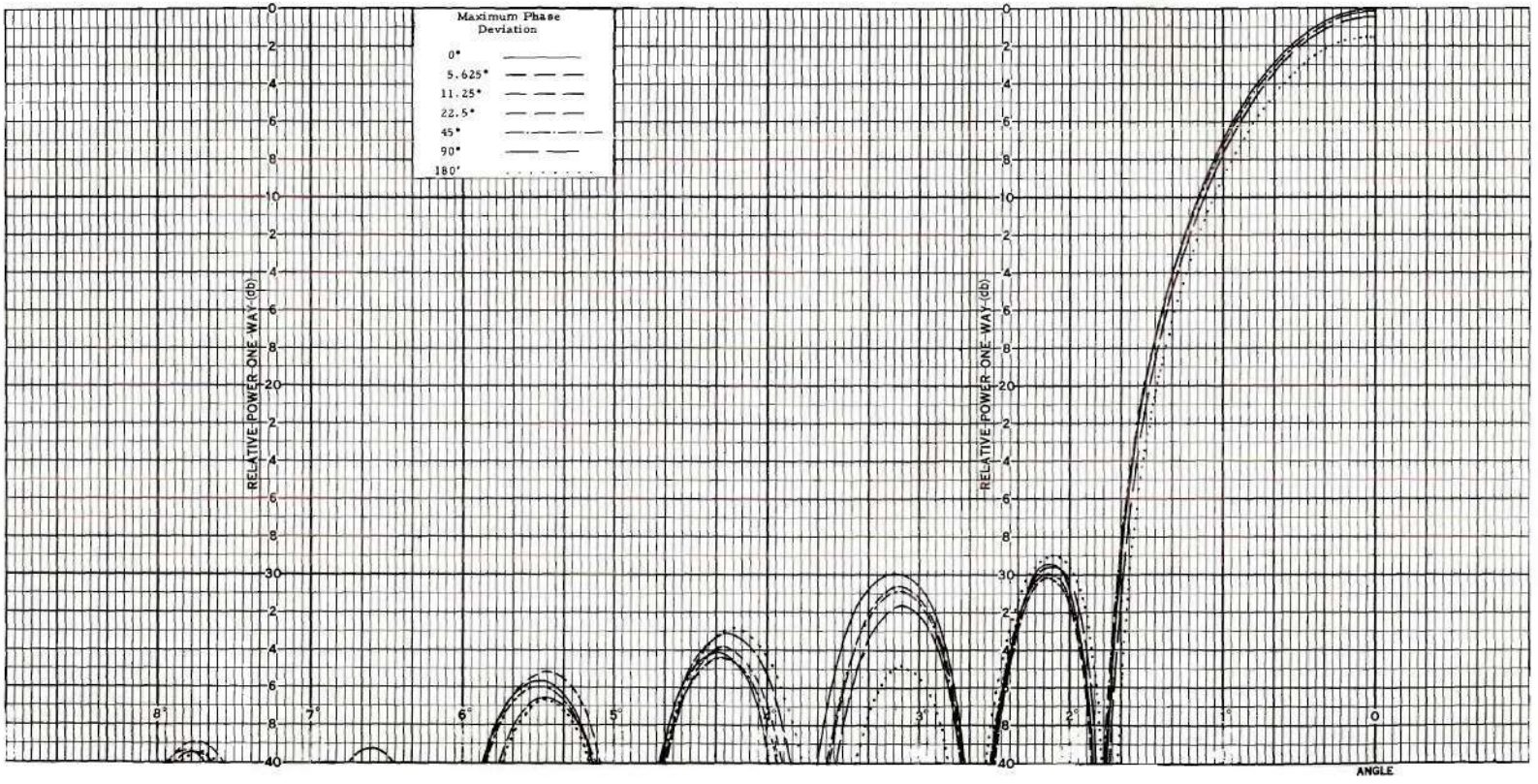

Figure 10. Patterns Computed in the y-z Plane for Case II

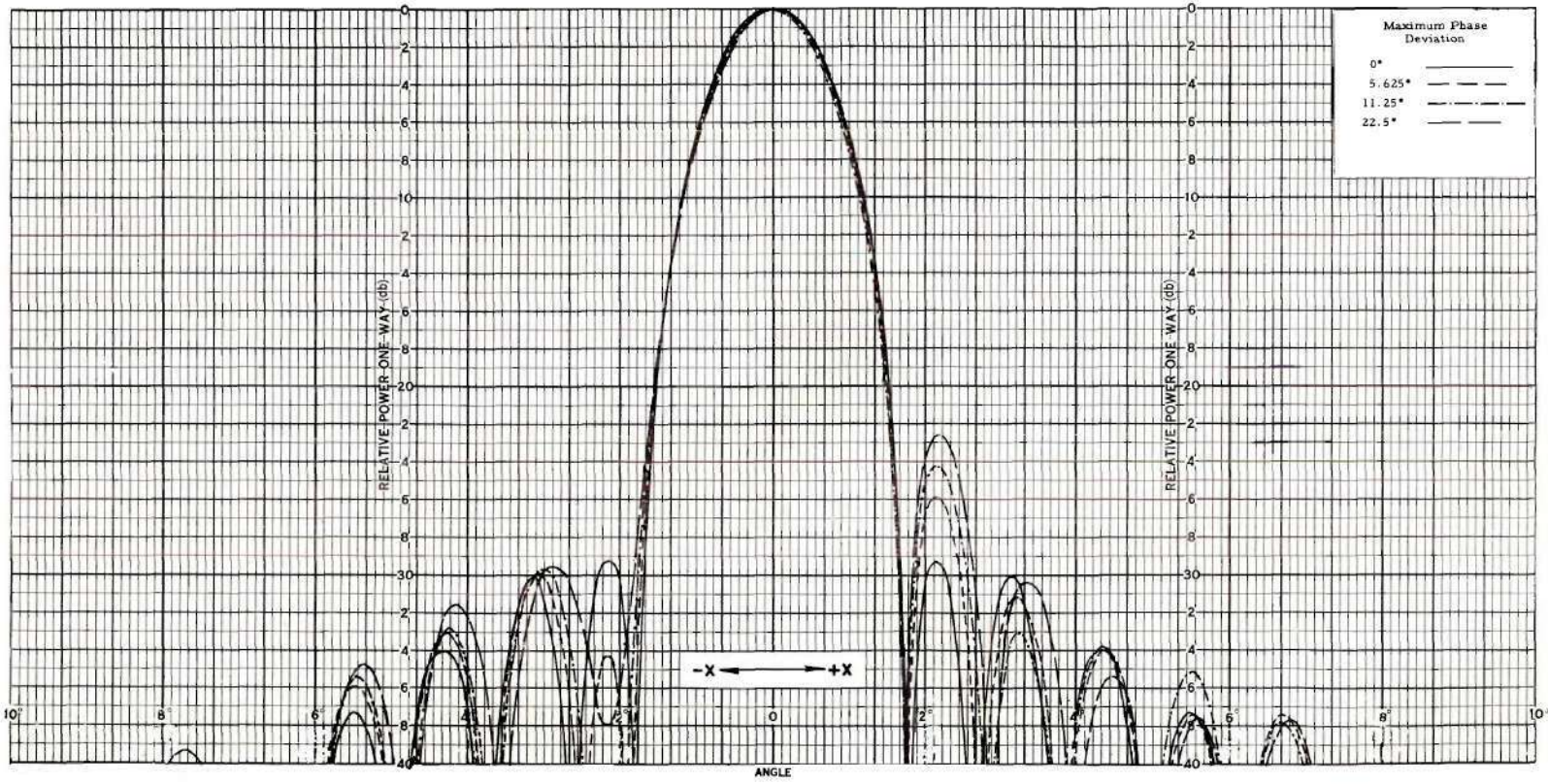

Figure 11. Patterns Computed in the x-z Plane for Case II

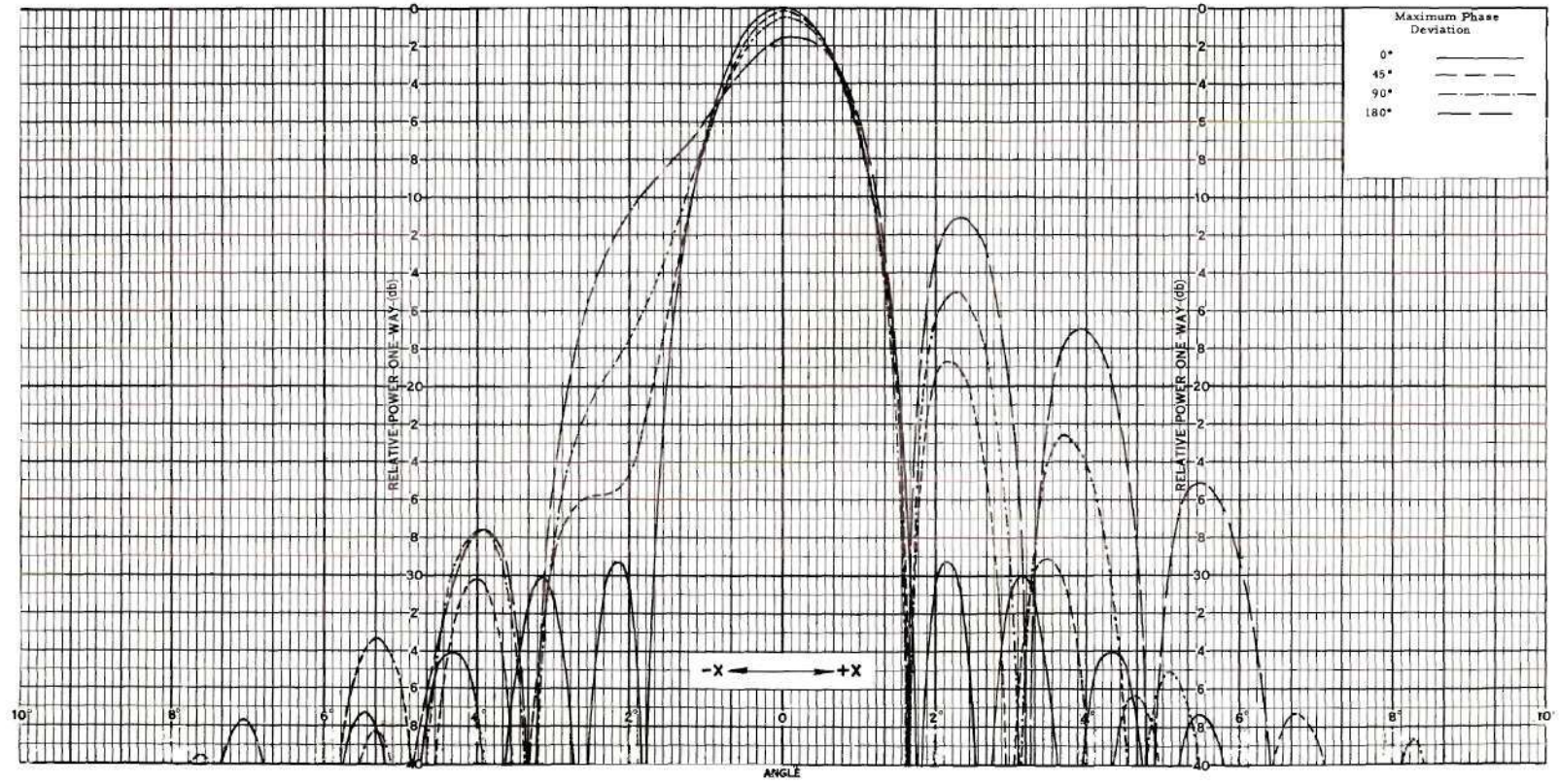

Figure 12. Patterns Computed in the x-z Plane for Case II (Continued)

CHAPTER VII

DISCUSSION OF RESULTS

Case I.--The antenna was considered to be exposed to different specified intensities of wind load, each of which was incident upon the antenna from the direction of the forward axis. From an examination of this physical problem, antenna distortions were defined which were considered to be characteristic of the actual distortions that would exist in the antenna. The far-field radiation patterns were computed, without difficulty, from the defined symmetrical characteristic reflectors with associated primary feeds. The antenna patterns computed formed a gradual transition away from the optimum for the sequence of increasing values of maximum aperture phase deviation. There are transitions in the peak magnitudes of the main lobe and first side lobe and in the degree of filling in the null between them from desirable to undesirable for the patterns computed for maximum aperture phase deviations of 11.25° and 22.5°.

Case II.--The antenna was considered to be exposed to different specified intensities of the wind load each of which was incident upon the antenna at an angle of 45° with respect to the forward axis direction. From an examination of this physical problem, antenna distortions were defined which were considered to be characteristic of the actual distortions that would exist in the antenna. From the defined asymmetrical characteristic reflectors with associated primary feeds, the

far-field radiation patterns were computed in two perpendicular planes, one of which was parallel to the incident direction of the wind load. For each plane considered, the antenna patterns computed formed a gradual transition away from the optimum for the sequence of increasing values of maximum aperture phase deviation. In the plane parallel to the incident load direction, there is a transition in the over-all pattern from desirable to undesirable between the patterns computed for maximum aperture phase deviations of 22.5° and 45°. Also, in the other plane a deterioration in the pattern occurs between the patterns computed for maximum aperture phase deviations of 22.5° and 45°. However, for this second plane the pattern changes are confined primarily to the main lobe.

CHAPTER VIII

CONCLUSIONS

With the application of the method of geometrical optics, simple relations were determined which are approximate solutions of the unmanageable expressions relating the distorted antennas considered with the respective aperture fields they produce. For both Cases I and II a linear relation existed between the maximum magnitude of distortion in the antenna and the maximum phase deviation in the field of the antenna aperture.

It is apparent that the method used to obtain the aperture fields of the distorted antennas can also be applied when other known antenna distortions exist providing these distortions are small in comparison with the dimensions of the antenna, and the distorted reflectors are both large and smooth compared with the wavelength of radiated energy. With the Fourier integral analog computer used to facilitate the computation of the far-field pattern from the aperture-field function, a technique is available with which a useful approximation to the radiation pattern of the distorted paraboloidal antenna can be obtained without prohibitive mathematical analysis. It is also apparent that for this type of distortion an analytical expression for the antenna distortion is not necessary in order to determine a useful approximation of the corresponding aperture field. It is only necessary for the distortion to be known at a sufficient number of points in the antenna.

With a procedure similar to that used in the illustrative examples, it would be possible to compute a sequence of far-field radiation patterns corresponding to a sequence of distorted antennas and from them determine the allowable distortion in the antenna for specified criteria in the far-field radiation pattern.

APPENDICES

APPENDIX I

THE TAYLOR DISTRIBUTION

The aperture field amplitude function defined to be present in the aperture of the paraboloidal antenna is the Taylor Distribution for a 30 db side lobe level and $\bar{n} = 4$ (14), where the maximum value of the distribution in the aperture is normalized to unity. The normalized symmetrical aperture amplitude distribution is computed at twenty equally spaced points outward along a radius of the aperture.

Table 1. Computed Values of Aperture Amplitude Function

Radius	Field Strength	Radius	Field Strength
0	1		
1	0.996	11	0.601
2	0.989	12	0.541
3	0.974	13	0.483
4	0.949	14	0.433
5	0.919	15	0.390
6	0.880	16	0.354
7	0.835	17	0.324
8	0.782	18	0.307
9	0.724	19	0.296
10	0.664	20	0.292

APPENDIX II

FEED-POINT LOCATIONS IN THE ANTENNAS OF CASE II

With respect to Figure 6, the feed point associated with a reflector is assumed to be located 20 wavelengths from the origin on the line in the x-z plane that is normal to the reflector at the origin.

The slope with respect to the z-axis of the normal is found as follows. The slope of the tangent in the x-z plane at the origin is found from

$$z = \frac{x^2}{4f} + \frac{x}{12.5b} \tag{37}$$

where $f = 20\lambda$

$$|x| \leq 12.5\lambda.$$

The tangent slope is

$$M_o = 12.5b. \tag{38}$$

Therefore, the slope of the normal is

$$N_o = -1/12.5b. \tag{39}$$

For $b > 2$ the feed point location is approximately $20/12.5b$ wavelengths in the negative x direction from its undistorted position. Thus, the deviation is

$$\delta x \cong -\frac{1.6\lambda}{b}. \tag{40}$$

APPENDIX III

THE DERIVATION OF Δz FOR CASE II

With reference to Figure 6, Δz is found from

$$d' + (f - z) + \Delta z = 2f. \tag{41}$$

Then
$$\Delta z = f + z - d'. \tag{42}$$

In Case II,

$$z = \frac{x^2 + y^2}{4f} + \left(\frac{2\lambda}{b}\right)\left(\frac{25\lambda - |y|}{25\lambda}\right)\left(\frac{x}{\sqrt{625\lambda^2 - y^2}}\right) \tag{43}$$

for
$$0 \leqq |x| \leqq \frac{\sqrt{625\lambda^2 - y^2}}{2}$$

where
$$f = 20\lambda$$

$$0 \leqq |y| \leqq 25\lambda.$$

If $b > 2$,

$$d' = \sqrt{(x - \delta x)^2 + y^2 + (f - z)^2}\ . \tag{44}$$

Substituting Equation 43 into Equation 44,

$$d' = \left[x^2 + y^2 + \left(f - \frac{x^2 + y^2}{4f}\right)^2 + \left(\frac{4\lambda^2}{b^2}\right)\left(\frac{25\lambda - |y|}{25\lambda}\right)^2 \right. \tag{45}$$

$$\left(\frac{x}{625\lambda^2 - y^2}\right)^2 - 2x \cdot \delta x + \delta x^2 -$$

$$\left.\left(\frac{4\lambda}{b}\right)\left(\frac{25\lambda - |y|}{25\lambda}\right)\sqrt{\frac{x}{625\lambda^2 - y^2}}\left(f - \frac{x^2 + y^2}{4f}\right)\right]^{1/2}.$$

The distance from the focal point of the paraboloidal reflector to any point on the reflector is

$$d = \left[x^2 + y^2 + \left(f - \frac{x^2 + y^2}{4f} \right)^2 \right]^{1/2} . \qquad (46)$$

For a maximum phase deviation of 180° or less in the aperture of the antennas of Case II, the magnitude of the difference between d and d' in Equation 45 is less than $\lambda/2$. Then d' is approximated by the first two terms of the binomial expansion

$$(X + Y)^{1/2} = X^{1/2} + \frac{1}{2} X^{-1/2} Y + \left(\frac{1}{2} \right) \left(-\frac{1}{2} \right) \frac{X^{-3/2} Y^2}{2!} + \cdots \qquad (47)$$

where $X = x^2 + y^2 + \left(f - \frac{x^2 + y^2}{4f} \right)^2 = \left(\frac{x^2 + y^2}{4f} + f \right)^2 = d^2$

and $Y = \left(\frac{4\lambda^2}{b^2} \right) \left(\frac{25\lambda - |y|}{25\lambda} \right)^2 \left(\frac{x}{625\lambda^2 - y^2} \right)^2 - 2x \cdot \delta x +$

$$\delta x^2 - \left(\frac{4\lambda}{b} \right) \left(\frac{25\lambda - |y|}{25\lambda} \right) \left(\frac{x}{625\lambda^2 - y^2} \right) \left(f - \frac{x^2 + y^2}{4f} \right).$$

Then

$$d' \cong \left(\frac{x^2 + y^2}{4f} + f \right) + \frac{\left(\frac{4\lambda^2}{b^2} \right) \left(\frac{25\lambda - |y|}{25\lambda} \right)^2 \left(\frac{x}{\sqrt{625\lambda^2 - y^2}} \right)^2}{2 \left(\frac{x^2 + y^2}{4f} + f \right)} + \qquad (48)$$

$$\frac{\left(\frac{4\lambda}{b} \right) \left(\frac{25\lambda - |y|}{25\lambda} \right) \left(\frac{x}{\sqrt{625\lambda^2 - y^2}} \right) \left(\frac{x^2 + y^2}{4f} - f \right) - 2x \cdot \delta x + \delta x^2}{2 \left(\frac{x^2 + y^2}{4f} + f \right)} .$$

Substituting Equations 43 and 48 into Equation 42, Δz reduces to

$$\Delta z \cong \frac{\frac{16\lambda f^2}{b}\left(\frac{x}{25\lambda}\right)\sqrt{\frac{25\lambda - |y|}{25\lambda + |y|}} + 4fx\cdot\delta x}{x^2 + y^2 + 4f^2} - \frac{\frac{8\lambda^2 f}{b^2}\left(\frac{x}{25\lambda}\right)^2\left(\frac{25\lambda - |y|}{25\lambda + |y|}\right) + 2f\cdot\delta x^2}{x^2 + y^2 + 4f^2} . \tag{49}$$

For $0 \leq |x| \leq \sqrt{625\lambda^2 - y^2}$, $0 \leq |y| \leq 25\lambda$, $f = 20\lambda$, and $b > 2$, Δz may be further approximated by

$$\Delta z \cong \frac{\frac{16f^2\lambda}{b}\left(\frac{x}{25\lambda}\right)\sqrt{\frac{25\lambda - |y|}{25\lambda + |y|}} + 4fx\cdot\delta x}{x^2 + y^2 + 4f^2} . \tag{50}$$

A procedure similar to the one leading to Equation 50 gives Equations 35 and 36. From Equations 50, 35, and 36, the maximum and minimum values of Δz for a given value of b occur at the aperture points $x = \mp 25\lambda$, $y = 0$, respectively. At $x = -25\lambda$, $y = 0$,

$$\Delta z \cong \frac{1.44\lambda}{b} , \tag{51}$$

and at $x = +25\lambda$, $y = 0$,

$$\Delta z \cong -\frac{1.44\lambda}{b} . \tag{52}$$

A maximum phase deviation of 180° in the aperture would be produced by $\Delta z = +\lambda/4$ at $x = -25\lambda$, $y = 0$ and $\Delta z = -\lambda/4$ at $x = +25\lambda$, $y = 0$. Referring to either Equation 51 or Equation 52, $b \cong 5.76$. Therefore,

for a maximum phase deviation of 180° or less in the apertures of the antennas of Case II, $b \gtrapprox 5.76$ This final condition on b indicates that the assumption $b > 2$ made in the derivation of Δz for Case II is valid.

APPENDIX IV

APPROXIMATE VALUES OF b FOR SELECTED VALUES OF MAXIMUM APERTURE PHASE DEVIATION

Case I.

$$\Delta z \cong \frac{1}{b}\left(\frac{128\lambda^2|x|}{x^2 + 1600}\right). \tag{53}$$

The maximum and minimum values of $128|x|\lambda^2/x^2 + 1600$ are respectively 1.438λ at $|x| = 25\lambda$ and 0 at $|x| = 0$. Therefore, the approximate values of b corresponding to selected values of aperture phase deviation are computed from

$$b \cong \frac{1.438\lambda}{\Delta z]_{|x| = 25\lambda}} \tag{54}$$

Table 2. Computed Values of b for Case I

Δz $\|x\| = 25\lambda$	Maximum Phase Deviation (Degrees)	Approximate Values of b
$\lambda/2$	180	2.876
$\lambda/4$	90	2 x "
$\lambda/8$	45	4 x "
$\lambda/16$	22.5	8 x "
$\lambda/32$	11.25	16 x "
$\lambda/64$	5.625	32 x "

Case II.

The approximate values of b corresponding to the selected values of aperture phase deviation are computed from

$$b \simeq \frac{1.44\lambda}{\Delta z]_{\substack{x = -25\lambda \\ y = 0}}} \tag{55}$$

Table 3. Computed Values of b for Case II

$\Delta z]_{\substack{x = -25\lambda \\ y = 0}}$	Maximum Phase Deviation (Degrees)	Approximate Values of b
$\lambda/4$	180	5.76
$\lambda/8$	90	2 x "
$\lambda/16$	45	4 x "
$\lambda/32$	22.5	8 x "
$\lambda/64$	11.25	16 x "
$\lambda/128$	5.625	32 x "

APPENDIX V

DATA FOR THE COMPUTATION OF APERTURE PHASE IN CASES I AND II

Case I.--The function $b\Delta z = 128\ |x|\ \lambda^2/x^2 + 1600$ was computed for eleven equally spaced points along the x-axis of Figure 7. The computed results are shown in Table 4.

Case II.--The function $b\Delta z$ was computed for values of x along the lines defined in the antenna aperture of Figure 6 by $|y| = 0,\ 2.5\lambda,\ 5\lambda,\ ---,\ 20\lambda,\ 22.5\lambda$, and 25λ. The computed results are shown in Table 5.

Table 4. Computed Values of $b\Delta z$ for Case I

x (wavelengths)	$b\Delta z$ (wavelengths)
0	0
2.5	0.199
5	0.394
7.5	0.579
10	0.753
12.5	0.911
15	1.052
17.5	1.175
20	1.280
22.5	1.367
25	1.438

Table 5. Computed Values of $b\Delta z$ for Case II

$\lvert y \rvert = 0\lambda$		$\lvert y \rvert = 2.5\lambda$	
$x_{(\lambda)}$	$b\Delta z_{(\lambda)}$	$x_{(\lambda)}$	$b\Delta z_{(\lambda)}$
0	0	0	0
± 2.5	± 0.200	± 2.5	± 0.160
± 5	± 0.395	± 5	± 0.315
± 7.5	± 0.580	± 7.5	± 0.463
± 10	± 0.750	± 10	± 0.602
± 12.5	± 0.910	± 12.45	± 0.726
± 15	± 0.350	± 15	± 0.200
± 17.5	∓ 0.175	± 17.5	∓ 0.290
± 20	∓ 0.640	± 20	∓ 0.710
± 22.5	∓ 1.07	± 22.5	∓ 1.09
± 25	∓ 1.44	± 24.9	∓ 1.43

$\lvert y \rvert = 5\lambda$		$\lvert y \rvert = 7.5\lambda$	
$x_{(\lambda)}$	$b\Delta z_{(\lambda)}$	$x_{(\lambda)}$	$b\Delta z_{(\lambda)}$
0	0	0	0
± 2.5	± 0.124	± 2.5	± 0.09
± 5	± 0.244	± 5	± 0.178
± 7.5	± 0.360	± 7.5	± 0.262
± 10	± 0.468	± 10	± 0.342
± 12.25	± 0.556	± 11.9	± 0.395
± 15	± 0.040	± 12.5	± 0.275
± 17.5	∓ 0.400	± 15	∓ 0.160
± 20	∓ 0.790	± 17.5	∓ 0.550
± 22.5	∓ 1.16	± 20	∓ 0.920
± 24.5	∓ 1.41	± 22.5	∓ 1.23
		± 23.85	∓ 1.38

Table 5 (Continued)

$\lvert y \rvert = 10\lambda$		$\lvert y \rvert = 12.5\lambda$	
$x_{(\lambda)}$	$b\Delta z_{(\lambda)}$	$x_{(\lambda)}$	$b\Delta z_{(\lambda)}$
0	0	0	0
± 2.5	± 0.058	± 2.5	± 0.028
± 5	± 0.115	± 5	± 0.056
± 7.5	± 0.168	± 7.5	± 0.083
± 10	± 0.219	± 10.8	± 0.115
± 11.45	± 0.247	± 12.5	∓ 0.136
± 12.5	± 0.065	± 15	∓ 0.478
± 15	∓ 0.305	± 17.5	∓ 0.800
± 17.5	∓ 0.670	± 20	∓ 1.06
± 20	∓ 0.990	± 21.65	∓ 1.25
± 22.9	∓ 1.32		

$\lvert y \rvert = 15\lambda$		$\lvert y \rvert = 17.5\lambda$	
$x_{(\lambda)}$	$b\Delta z_{(\lambda)}$	$x_{(\lambda)}$	$b\Delta z_{(\lambda)}$
0	0	0	0
± 2.5	0	± 2.5	∓ 0.026
± 5	0	± 5	∓ 0.052
± 7.5	0	± 7.5	∓ 0.076
± 10	0	± 8.93	∓ 0.090
± 12.5	∓ 0.328	± 10	∓ 0.211
± 15	∓ 0.628	± 12.5	∓ 0.483
± 17.5	∓ 0.900	± 15	∓ 0.738
± 20	∓ 1.15	± 17.85	∓ 1.00

Table 5 (Continued)

$\lvert y \rvert = 20\lambda$		$\lvert y \rvert = 22.5\lambda$	
$x_{(\lambda)}$	$b\Delta z_{(\lambda)}$	$x_{(\lambda)}$	$b\Delta z_{(\lambda)}$
0	0	0	0
± 2.5	∓ 0.054	± 2.5	∓ 0.082
± 5	∓ 0.105	± 5	∓ 0.163
± 7.5	∓ 0.156	± 5.45	∓ 0.177
± 10	∓ 0.407	± 7.5	∓ 0.350
± 12.5	∓ 0.645	± 10	∓ 0.558
± 15	∓ 0.864	± 10.9	∓ 0.627

$\lvert y \rvert = 25\lambda$	
$x_{(\lambda)}$	$b\Delta z_{(\lambda)}$
0	0

APPENDIX VI

EQUIVALENT SLIT APERTURE FUNCTIONS FOR CASES I AND II

Case I.--The x-z equivalent slit aperture functions for the antennas considered in Case I are shown in Table 6.

Case II.--The y-z equivalent slit aperture functions for the antennas considered in Case II are shown in Table 7. The x-z equivalent slit aperture functions for the antennas considered in Case II are shown in Table 8 where the values of the functions at $x = -2.5\lambda$ through -22.5λ are unchanged from the values at $x = +2.5\lambda$ through $+22.5\lambda$ except for the sign of the phase components.

Table 6. Equivalent Slit Aperture Functions for Case I

Aperture Cuts, $\lvert x \rvert$ in Wavelengths	Magnitude of Maximum Aperture Phase Deviation is 0°		Magnitude of Maximum Aperture Phase Deviation is 5.625°	
	Normalized Magnitude	Phase in Degrees	Normalized Magnitude	Phase in Degrees
0	1	0	0.998	2.5
2.5	0.995	0	0.994	4.0
5	0.933	0	0.932	4.5
7.5	0.860	0	0.860	3.5
10	0.757	0	0.757	3.0
12.5	0.626	0	0.625	3.0
15	0.518	0	0.518	4.5
17.5	0.408	0	0.408	6.5
20	0.299	0	0.299	6.5
22.5	0.200	0	0.200	5.0

Aperture Cuts, $\lvert x \rvert$ in Wavelengths	Magnitude of Maximum Aperture Phase Deviation is 11.25°		Magnitude of Maximum Aperture Phase Deviation is 22.5°	
	Normalized Magnitude	Phase in Degrees	Normalized Magnitude	Phase in Degrees
0	0.998	6.0	0.993	11.0
2.5	0.990	6.0	0.988	11.5
5	0.935	6.0	0.932	12.5
7.5	0.860	7.5	0.859	13.5
10	0.757	8.0	0.756	13.5
12.5	0.625	7.5	0.625	15.5
15	0.518	9.5	0.518	19.5
17.5	0.408	11.5	0.407	21.5
20	0.299	11.0	0.299	21.5
22.5	0.200	10.5	0.200	20.0

Table 6 (Continued)

Aperture Cuts, $\|x\|$ in Wavelengths	Magnitude of Maximum Aperture Phase Deviation is 45°		Magnitude of Maximum Aperture Phase Deviation is 90°	
	Normalized Magnitude	Phase in Degrees	Normalized Magnitude	Phase in Degrees
0	0.974	20.5	0.898	41.5
2.5	0.973	22.5	0.920	44.0
5	0.923	24.0	0.887	48.0
7.5	0.850	27.5	0.812	54.5
10	0.753	32.0	0.742	61.5
12.5	0.623	32.5	0.620	66.5
15	0.517	36.5	0.512	72.5
17.5	0.406	39.5	0.405	79.0
20	0.298	41.5	0.292	82.0
22.5	0.198	42.0	0.193	85.0

Aperture Cuts, $\|x\|$ in Wavelengths	Magnitude of Maximum Aperture Phase Deviation is 180°	
	Normalized Magnitude	Phase in Degrees
0	0.633	81.5
2.5	0.719	85.0
5	0.738	94.5
7.5	0.718	108.0
10	0.682	122.0
12.5	0.590	133.0
15	0.491	145.5
17.5	0.397	157.0
20	0.295	165.0
22.5	0.192	172.0

Table 7. y-z Equivalent Slit Aperture Functions for Case II

Aperture Cuts, $\|y\|$ in Wavelengths	Magnitude of Maximum Aperture Phase Deviation is 0°		Magnitude of Maximum Aperture Phase Deviation is 5.625°	
	Normalized Magnitude	Phase in Degrees	Normalized Magnitude	Phase in Degrees
0	1		1	
2.5	0.992		0.991	
5	0.917	Phase	0.917	Phase
7.5	0.856		0.856	
10	0.750	is	0.750	is
12.5	0.628		0.628	
15	0.512	Zero	0.512	Zero
17.5	0.404		0.404	
20	0.300		0.300	
22.5	0.202		0.202	

Aperture Cuts, $\|y\|$ in Wavelengths	Magnitude of Maximum Aperture Phase Deviation is 11.25°		Magnitude of Maximum Aperture Phase Deviation is 22.5°	
	Normalized Magnitude	Phase in Degrees	Normalized Magnitude	Phase in Degrees
0	1		0.998	
2.5	0.991		0.990	
5	0.916	Phase	0.916	Phase
7.5	0.855		0.854	
10	0.750	is	0.750	is
12.5	0.628		0.627	
15	0.512	Zero	0.511	Zero
11.5	0.404		0.404	
20	0.300		0.300	
22.5	0.202		0.202	

Table 7 (Continued)

Aperture Cuts, $\lvert y \rvert$ in Wavelengths	Magnitude of Maximum Aperture Phase Deviation is 45°		Magnitude of Maximum Aperture Phase Deviation is 90°	
	Normalized Magnitude	Phase in Degrees	Normalized Magnitude	Phase in Degrees
0	0.988		0.952	
2.5	0.983	Phase	0.956	Phase
5	0.910		0.892	
7.5	0.850	is	0.832	is
10	0.749		0.732	
12.5	0.623	Zero	0.613	Zero
15	0.510		0.500	
17.5	0.403		0.397	
20	0.300		0.293	
22.5	0.202		0.200	

Aperture Cuts, $\lvert y \rvert$ in Wavelengths	Magnitude of Maximum Aperture Phase Deviation is 180°	
	Normalized Magnitude	Phase in Degrees
0	0.814	
2.5	0.846	Phase
5	0.820	
7.5	0.766	is
10	0.680	
12.5	0.571	Zero
15	0.465	
17.5	0.370	
20	0.276	
22.5	0.192	

Table 8. x-z Equivalent Slit Aperture Functions for Case II

Aperture Cuts, x in Wavelengths	Magnitude of Maximum Aperture Phase Deviation is 0°		Magnitude of Maximum Aperture Phase Deviation is 5.625°	
	Normalized Magnitude	Phase in Degrees	Normalized Magnitude	Phase in Degrees
0	1	0	1	0
2.5	0.994	0	0.994	0.0
5	0.935	0	0.935	1.0
7.5	0.858	0	0.858	1.0
10	0.752	0	0.752	1.0
12.5	0.628	0	0.628	1.0
15	0.515	0	0.514	0.0
17.5	0.404	0	0.404	-1.0
20	0.300	0	0.300	-2.0
22.5	0.201	0	0.201	-2.0

Aperture Cuts, x in Wavelengths	Magnitude of Maximum Aperture Phase Deviation is 11.25°		Magnitude of Maximum Aperture Phase Deviation is 22.5°	
	Normalized Magnitude	Phase in Degrees	Normalized Magnitude	Phase in Degrees
0	1	0	1	0
2.5	0.994	1.0	0.994	1.5
5	0.935	1.0	0.934	2.0
7.5	0.857	1.5	0.857	2.5
10	0.752	1.0	0.751	2.0
12.5	0.627	1.0	0.625	1.5
15	0.514	-1.0	0.514	-2.0
17.5	0.404	-2.0	0.403	-4.0
20	0.300	-4.0	0.300	-7.5
22.5	0.201	-4.0	0.201	-8.0

Table 8 (Continued)

Aperture Cuts, x in Wavelengths	Magnitude of Maximum Aperture Phase Deviation is 45°		Magnitude of Maximum Aperture Phase Deviation is 90°	
	Normalized Magnitude	Phase in Degrees	Normalized Magnitude	Phase in Degrees
0	1	0	1	0
2.5	0.994	2.5	0.993	3.0
5	0.933	3.0	0.927	4.5
7.5	0.855	4.0	0.849	7.0
10	0.750	4.0	0.740	8.0
12.5	0.621	2.5	0.605	5.0
15	0.512	- 4.0	0.504	- 7.0
17.5	0.402	- 8.5	0.400	-17.0
20	0.300	-15.0	0.299	-29.5
22.5	0.200	-16.5	0.200	-36.0

Aperture Cuts, x in Wavelengths	Magnitude of Maximum Aperture Phase Deviation is 180°	
	Normalized Magnitude	Phase in Degrees
0	1	0
2.5	0.990	5.0
5	0.917	9.0
7.5	0.822	14.0
10	0.699	16.0
12.5	0.543	10.5
15	0.476	-13.5
17.5	0.391	-36.0
20	0.294	-57.0
22.5	0.198	-73.0

BIBLIOGRAPHY

1. Ruze, J., Physical Limitations on Antennas, Unpublished Ph.D. Thesis, Massachusetts Institute of Technology, 1952. Also in Technical Report 248, Research Laboratory of Electronics, Massachusetts Institute of Technology, 1952.

2. Jordan, E. C., Electromagnetic Waves and Radiating Systems, New Jersey, Prentice-Hall, Inc., 1950, pp. 555-63.

3. Silver, S., Microwave Antenna Theory and Design, New York, McGraw-Hill Book Company, Inc., 1949, pp. 119-22.

4. Ibid, p. 122.

5. Ibid, p. 139.

6. Ibid, p. 170.

7. Kraus, J. D., Antennas, New York, McGraw-Hill Book Company, Inc., 1950, pp. 347-8.

8. Campbell, G. A., and Foster, R. M., Fourier Integrals for Practical Applications, D. Van Nostrand Company, Inc., New York, 1948.

9. Silver, Op. Cit., pp. 170-4.

10. Moseley, R. E., Shaping Microwave Antenna Radiation Patterns by an Aperture-Field Method, Unpublished M.S. Thesis, Georgia Institute of Technology, 1959, p. 11.

11. Hollis, J. S., A Fourier Integral Computer for Calculation of Antenna Radiation Patterns, Unpublished M.S. Thesis, Georgia Institute of Technology, 1956.

12. Personal communication with Mr. J. S. Hollis of Scientific-Atlanta, Inc., Atlanta, Georgia, on September 6, 1960.

13. Taylor, T. T., "Design of Circular Apertures for Narrow Beamwidth and Low Sidelobes," Institute of Radio Engineers Transactions on Antennas and Propagation, Volume AP-8, Number 1, January 1960, pp. 17-22.

14. Hansen, R. C., "Tables of Taylor Distributions for Circular Aperture Antennas," Institute of Radio Engineers' Transactions on Antennas and Propagation, Volume AP-8, Number 1, January 1960, pp. 23-26.